Numerical Modelling of the Manukau Harbour Entrance: High-Level Estimates of Dredged Entrance Channel Infilling.

Prepared for

sapere

eCoast
eTakutai

MOHIO - AUAHA - TAUTOKO
UNDERSTAND - INNOVATE - SUSTAIN

PO Box 151, Raglan 3225, New Zealand
Ph: +64 7 825 0087 | info@ecoast.co.nz | www.ecoast.co.nz

Numerical Modelling of the Manukau Harbour Entrance: High-Level Estimates of Dredged Entrance Channel Infilling.

Report Status

Version	Date	Status	Approved by
V. 1	4 March 2020	Final Draft	STM

It is the responsibility of the reader to verify the version number of this report.

Authors

Shaw Mead *BSc, MSc (Hons), PhD*

Rhys McIntosh *BSc, MSc (Hons)*

Sam O'Neill *BSc, MSc (Hons)*

Dougal Greer *BSc, MSc (Hons)*

Contents

Figures

Tables

1 Background

This investigation leads on from the Ports Future Study (Ernst and Young, 2016), in which eCoast provided expertise in the areas of coastal processes and marine ecology in a process which worked from a long-list of over 20 potential options for the future Port of Auckland. The Manukau Harbour and 2 sites in the Firth of Thames were found to the be the preferred sites for a future Port of Auckland, and detailed analysis of existing information and estimates of the entrance channel were undertaken by eCoast. However, a great deal of uncertainty remained with respect to the requirements for maintenance dredging and the stability of the entrance channel through the ebb-tidal delta (i.e. the Manukau Bar). eCoast and the reviewers recommended that numerical modelling would provide a better insight into sedimentation rates and the requirements for maintenance dredging.

This report details uncalibrated numerical modelling that has been undertaken to provide an indication of sedimentation and the impact of extreme storm events on a dredged channel through the Manukau Bar, without a targeted fieldwork campaign[1]. In addition, in order to provide further insight into the interpretation of modelling results and likely maintenance requirements, along with the modelling of the Manukau Harbour entrance as described above, reviews of field investigations and numerical modelling of similar sites (in New Zealand and internationally) were undertaken to provide further information and understanding of the possible dredging regime.

1.1 Physical Setting

Manukau Harbour is a large (~370 km^2) shallow estuary situated on Auckland's west coast of the North Island, New Zealand (Figure 1.1). Its entrance, referred to as Manukau Heads, is 9 km long, ~2.2 km wide, has a ~30 m deep channel with an extensive ebb tidal delta system (bar) that extends ~5 km offshore. The ebb tidal delta has an estimated sediment volume of 1,250 x 10^6 m^3 (Hicks and Hume, 1996), with depths on the bar as shallow as 7 m. The inner harbour has an average depth of 6.1 m, and is characterised by a highly developed branching channel system, of which there are four main channels (Waiuku, Papakura, Purakau and Wairopa; Figure 1.3), that drain the intertidal flats (NIWA, 2007). At mean low spring tide, 40%

[1] A fieldwork campaign to develop a calibrated sediment transport model of the Manukau Harbour entrance will provide a greater level of confidence than an uncalibrated model, however, such a campaign would be expensive and take some years to complete. This initial modelling investigation has been undertaken in order to have a better understanding of the likely sedimentation before committing to such investigations.

of the surface area of the estuary is comprised of low-gradient intertidal flats (Heath *et al.*, 1977).

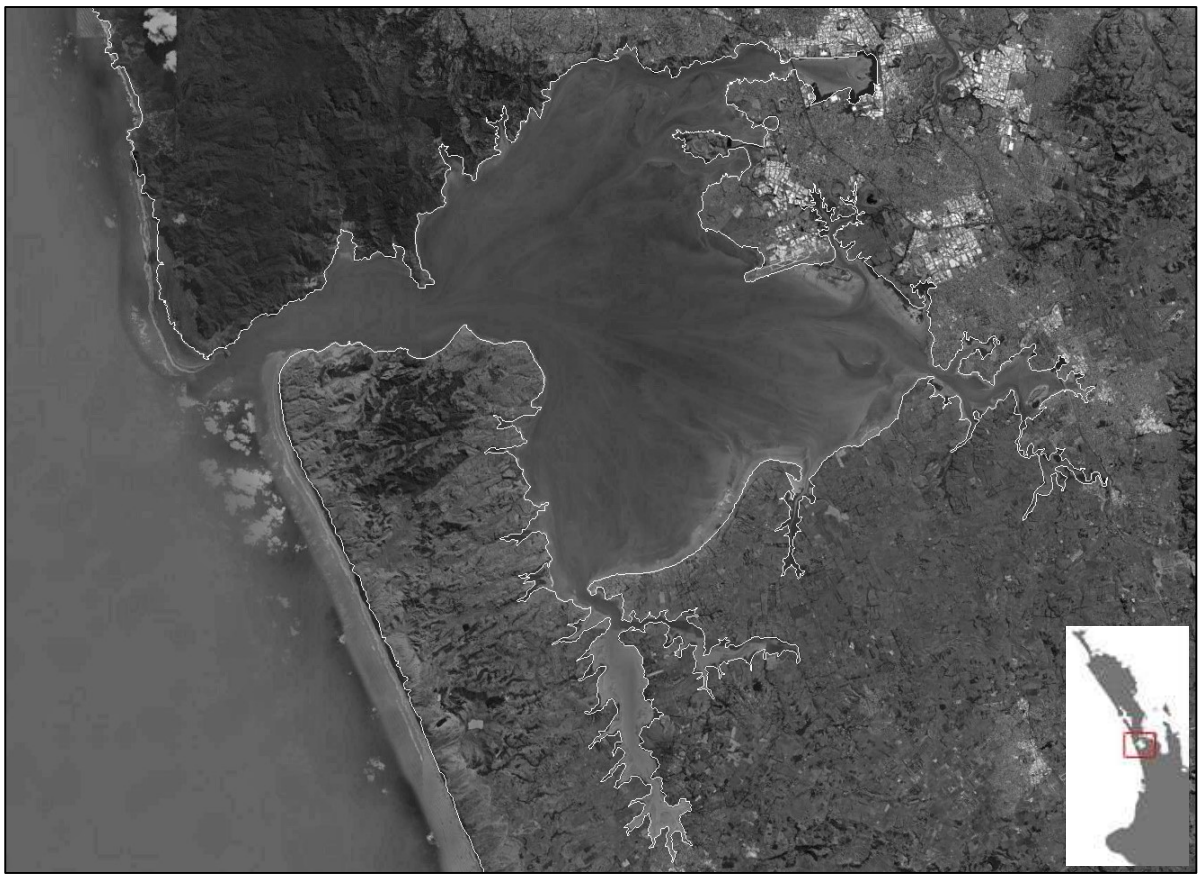

Figure 1.1. Map of Manukau Harbour.

The semi-diurnal tidal range in the Manukau Harbour at Onehunga Wharf (Figure 1.3) varies between 1.9 m and 3.4 m, from neap to spring tide respectively, translating to flow volumes of up to 918 million m^3 (Hicks and Hume, 1996). Freshwater input to the harbour is received from an 870 km^2 catchment via many small streams (Figure 1.2) and even after high rainfall events, this contribution is small when compared to the tidal prism. The residence time of water in the harbour based on salinity measurements ranges from 11 days (Vant and Williams, 1992) to 22 days (Heath *et al.*, 1977) with large spatial and seasonal variation. The water inside the harbour is well mixed with little vertical or horizontal salinity or temperature variation and the seabed morphology is primarily a function of tidally driven circulation. The morphology of the upper intertidal zone, however, largely results from the combination of wind-driven flow and locally generated wind-wave currents that act to suspend and transport fine sediments contributing to the high turbidity levels observed in the harbour (Bell *et al.*, 1998).

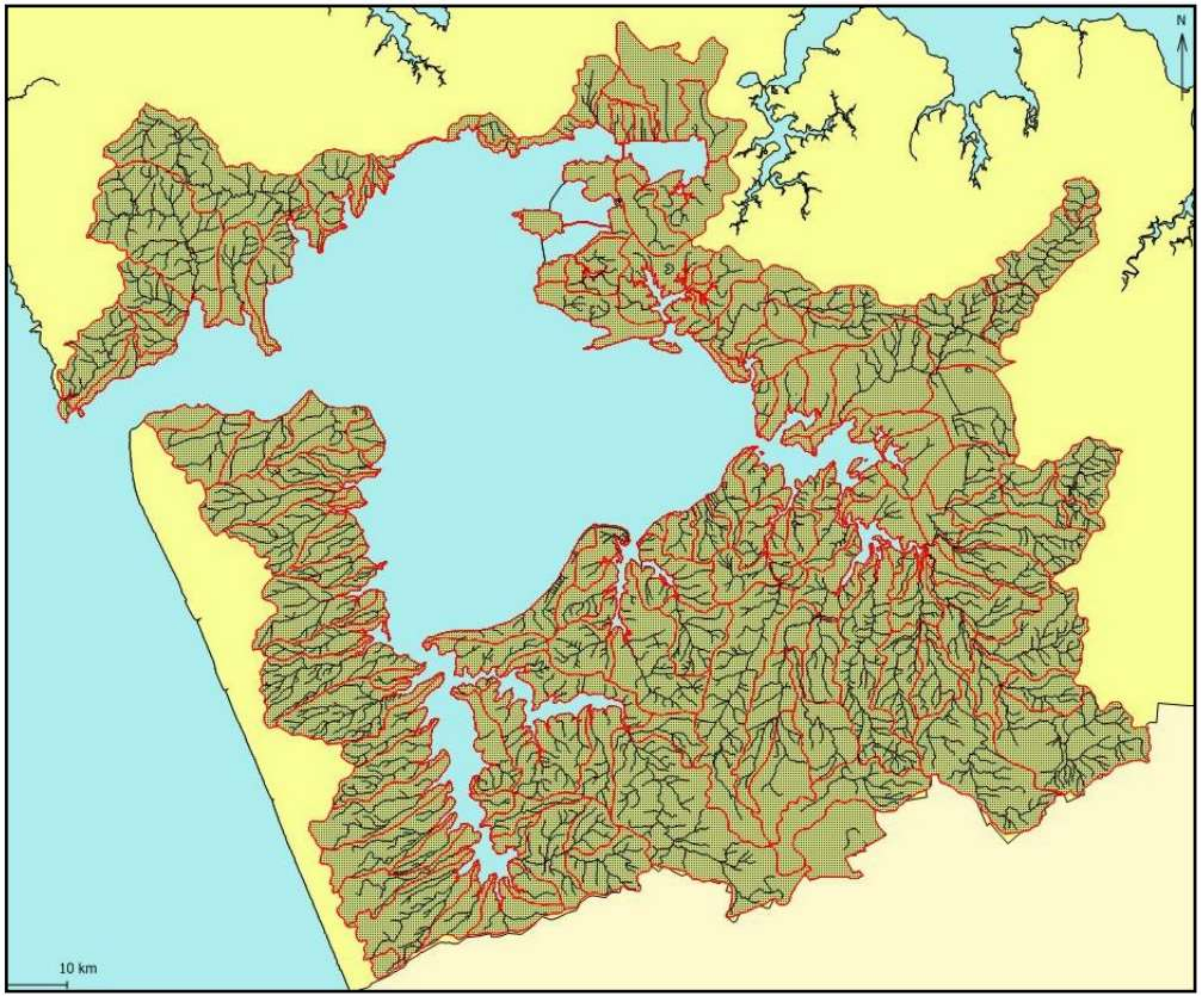

Figure 1.2. Manukau Harbour watershed, sub-catchments and fluvial systems (Kelly, 2008).

The inner harbour shoreline is complex with many side branches extending off the main body of the estuary (Figure 1.3), most of which are heavily forested with mangroves. These areas vary from highly modified to completely unmodified with large portions of the western and southern shores remaining relatively unmodified while urban coastal development has led to a significant transformation of the northern and eastern shorelines. In particular, Mangere Inlet has seen extensive coastal reclamation works to accommodate port activities and roading while to the south, Mangere Wastewater Treatment Plant (WTP) and Auckland International Airport are built on 500 ha and 66 ha of reclaimed intertidal flats, respectively (Figure 1.3). These modifications have led to the loss of many embayments and stream inlets.

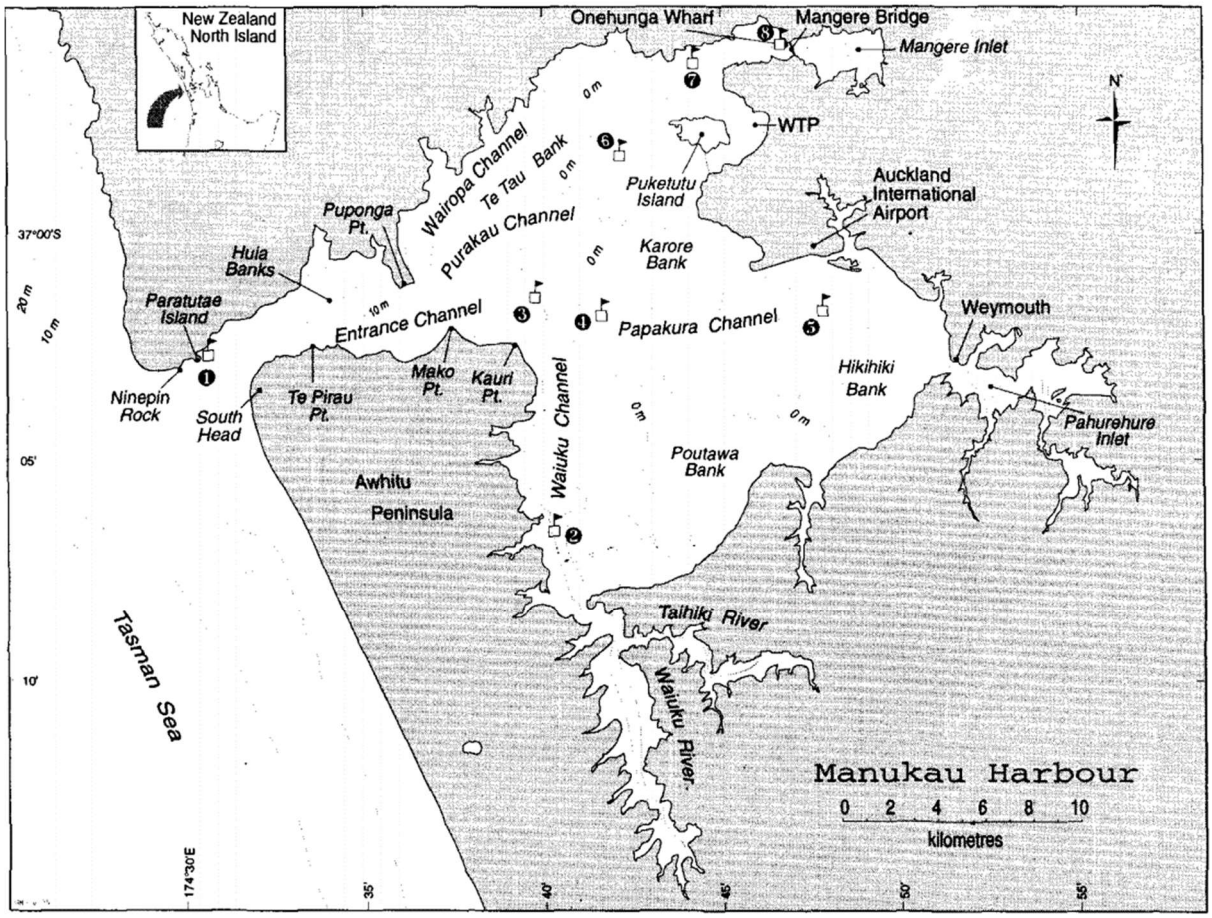

Figure 1.3. Channels, intertidal banks and major freshwater inlets/creeks of Manukau Harbour (Bell *et al.*, 1998).

1.2 Hydrodynamic Overview

Manukau Harbour has some of the largest tidal ranges in New Zealand (Hume *et al.*, 1992) which vary from 1.9 m to 3.4 m (neap to spring) at Onehunga Wharf. Tides are hydraulically amplified in the side branches and can have a range of up to 4.5 m in the Pahurehure Inlet (Pritchard *et al.*, 2008). With relatively little contribution from freshwater input, flows in the harbour are predominantly tidally driven. The most complex current regimes exist in the entrance channel where the major inner-harbour channels converge through the 2.2 km wide gap between Puponga Point and Mako Point (Figure 1.3). Peak current velocities can reach up to 2.25 m/s here, and are the strongest flows observed in the entire harbour (Heath *et al.*, 1977). A flood tidal delta known as the Huia Banks lies in the middle of the entrance channel and can get as shallow as 5 m below mean sea level (Figure 1.3). This feature presents an obstacle to the tidal flows and creates a convergence against the western side of Puponga Point where strong tidal currents occur. Residual current modelling conducted by Bell *et al.* (1998) revealed that there are consistent flood-directed residual flows along the northern flank of the Huia Banks and along the western side of Puponga Point. Additionally, large scale ebb-

directed residual flows occur on the eastern side of Puponga Point in the lower Wairopa Channel (Figure 1.4).

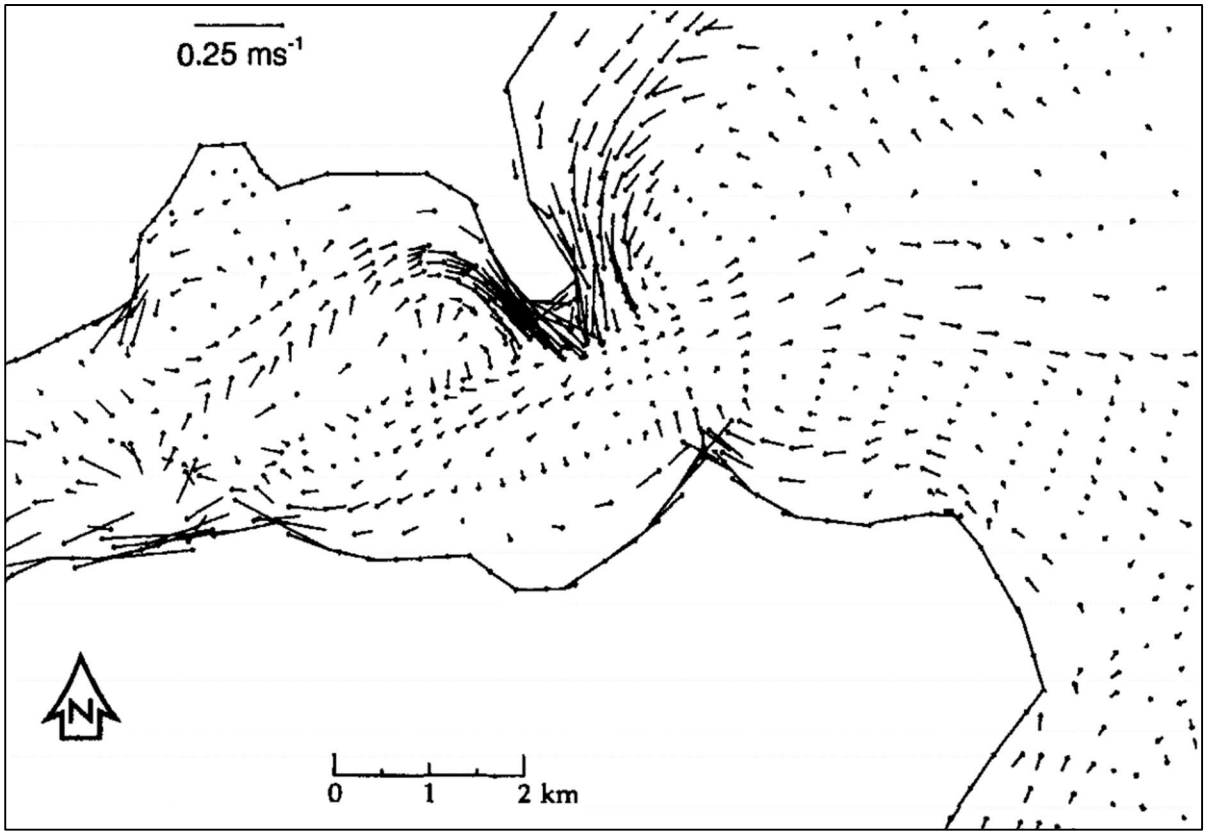

Figure 1.4. Residual currents in the Manukau Harbour entrance channel (Bell *et al.*, 1998).

There are no large-scale eddies in the Manukau Harbour due to the presence of the relatively deep and narrow channels and in addition to the entrance channel currents, strong flows occur in several other constricted inlets (Pritchard *et al.*, 2008). For example, spring tidal flows have been observed to exceed 1.0 m/s at the entrance to the Mangere Inlet and Pahurehure Inlet (Bell *et al.*, 1998).

There is some influence of wind driven circulation along with the effects of wind-wave generated currents throughout the estuary. These processes are widely dwarfed by the tidally driven flows, however, in the shallow upper-intertidal flats at high tide where tidal currents are weak, they become the primary driver of circulation (Smith *et al.*, 2001).

The paths followed by estuarine flood and ebb currents often differ with the channels carrying ebbing flows at low tide generally being ebb dominant, and have characteristic net seaward bed sediment transport (Murray North Ltd., 1988). On the contrary, channels that are terminated by a shoal at their landward end are flood dominant. Considerable volumes of

sediment can be exchanged between the ebb and flood dominated channels that continually changes their geometry through erosion and deposition. Sediments are redistributed all over the Manukau Harbour by this process.

1.3 Wave Climate

A long-term offshore wave climate was taken from a 0.5-degree by 0.5-degree global model of wave characteristics maintained by the U.S. National Oceanic and Atmospheric Administration (NOAA). The 40-year record runs from 1979 until 2019, although there are some gaps. The full record of data was extracted from the model from a point corresponding to -37.5° latitude and 174° longitude offshore of the Manukau Harbour entrance. The wave climate at this location is summarised in the wave roses shown in Figure 1.5, which indicates that the majority of waves come from the southwest. Significant wave heights (H_s) are mostly less than 3 m with peak periods (T_p) typically between 10 and 16 seconds.

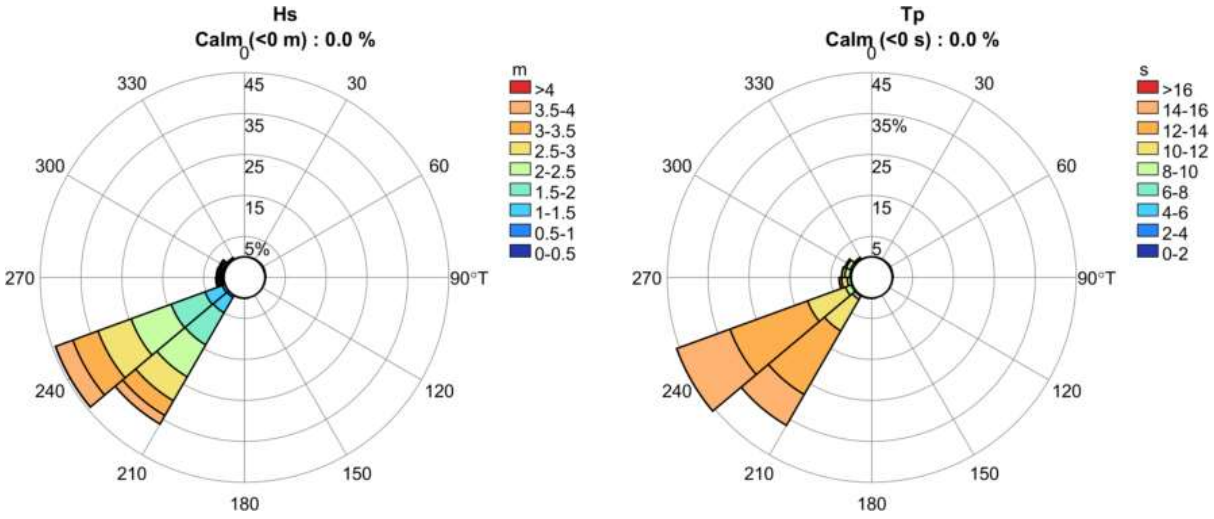

Figure 1.5. Roses of significant wave height (left) and peak period (right) offshore of Manukau Harbour (1979 - 2019).

Plotting H_s against T_p (Figure 1.6) shows that for low values of H_s there is a large range of values for T_p, however, for extreme events (>6 m), T_p is limited to being between 10 and 18 s. Plotting H_s against D_p (Figure 1.7) shows that the largest records come from the southwest/west (between 220 and 270 degrees).

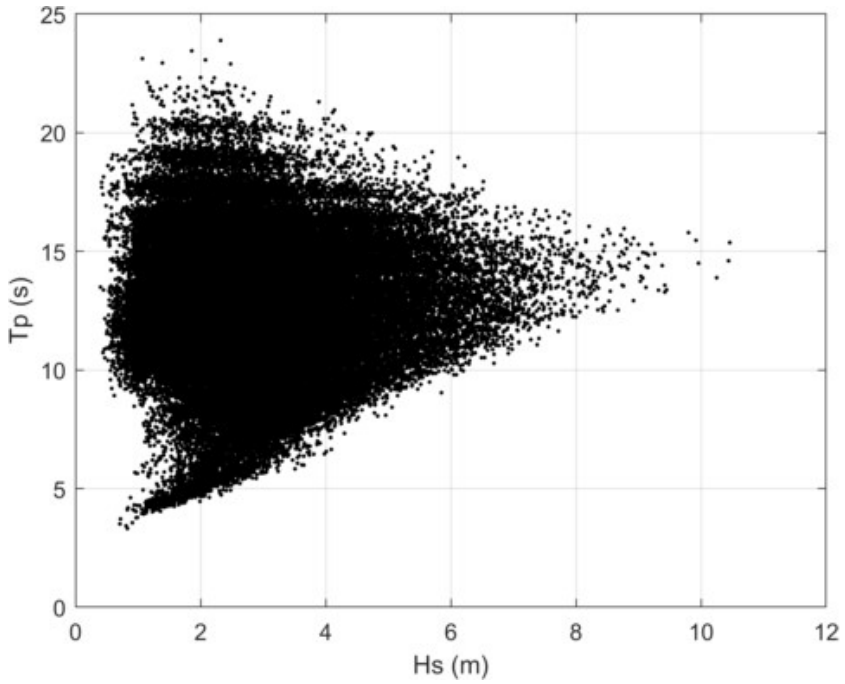

Figure 1.6. Plot of significant wave height vs. peak period offshore of Manukau Harbour (1979 - 2019).

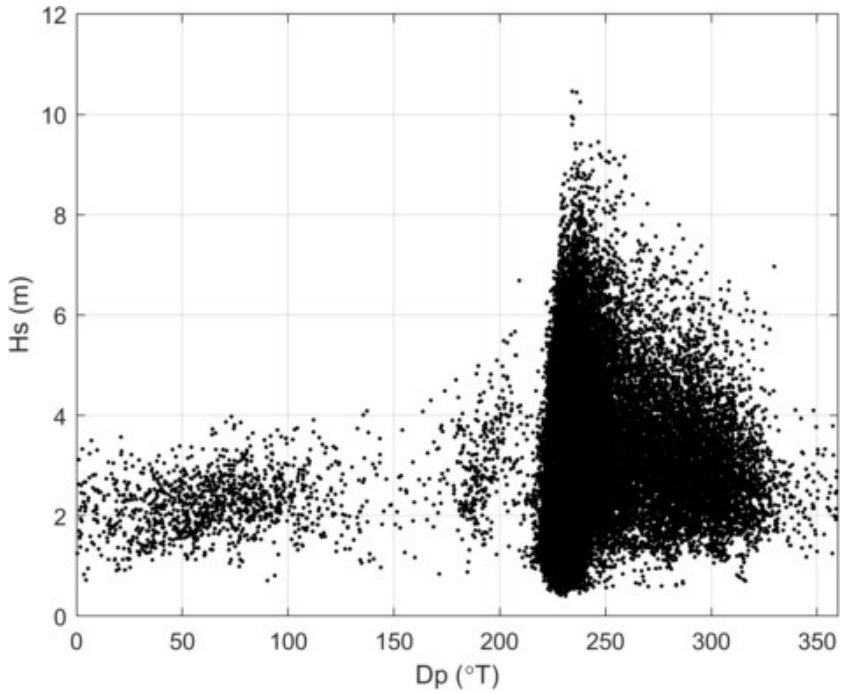

Figure 1.7. Plot of peak direction vs. significant wave height offshore of Manukau Harbour (1979 - 2019).

1.4 The Ebb Tidal Delta

In their study of 15 ebb tidal deltas around the top half of New Zealand's North Island, Hicks and Hume (1991) determined the volume and shape of the individual deltas using digital terrain modelling and by drawing comparisons with inferred 'no-delta' shoreface profiles.

Hicks and Hume (1991) used digitised hydrographic fair sheets from Royal New Zealand Navy surveys taken over the preceding 40 years. Three basic shapes of 'residual' ebb-delta were identified and were distinguished based the delta length/breadth ratio. The characteristics of each were shown to be related mainly to delta size and shoreline configuration (through its control on wave exposure), the space available for the delta to occupy, and the alignment of the ebb tidal jet. Based on their classification scheme, Hicks and Hume (1991) classified the Manukau ebb tidal delta as a Type I, that is, the shape of the ebb tidal delta can be described as longshore-elongated, reasonably symmetrical "batwing shaped", and they found this to be typical of relatively straight exposed shorelines experiencing significant littoral drift.

Though no quantitative analysis of the changing geometry and volume of the Manukau ebb tidal delta exists, Fairburn (1987) illustrated the changing shape of the ebb tidal delta through the period 1864 – 1958 at a decadal temporal scale (Figure 1.8). Furthermore, notes on Hydrographic Chart NZ4314 of Manukau Harbour state that shoals and depths in the approaches to the entrance channel are constantly changing. All indications are that the ebb tidal delta is in a state of dynamic equilibrium and its shape and the associated orientation of the ebb jet ("Middle Deep" in Figure 1.8) at any given time are in response to longshore sediment supply, incident wave conditions, estuarine sediment supply and tidal forcing.

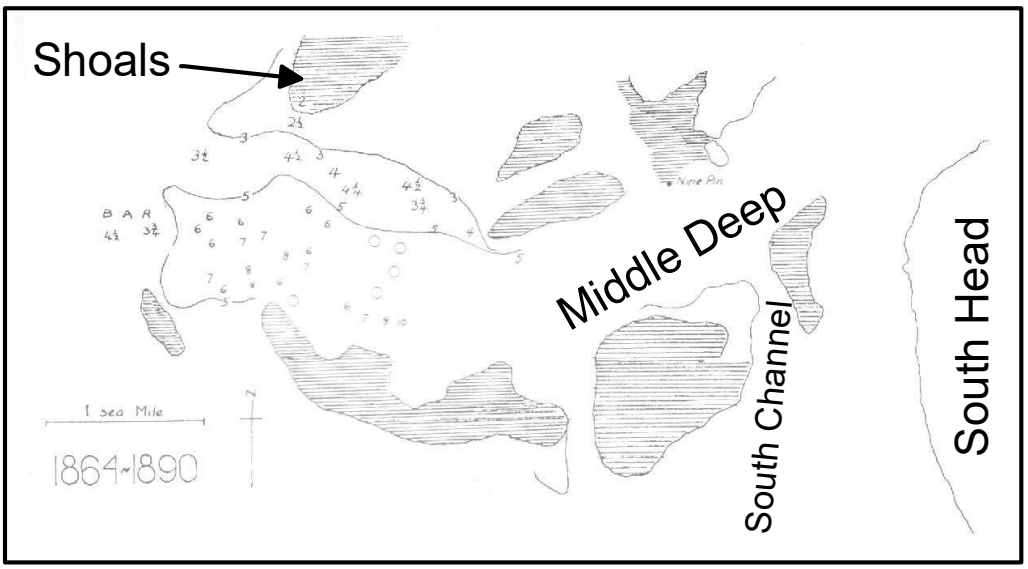

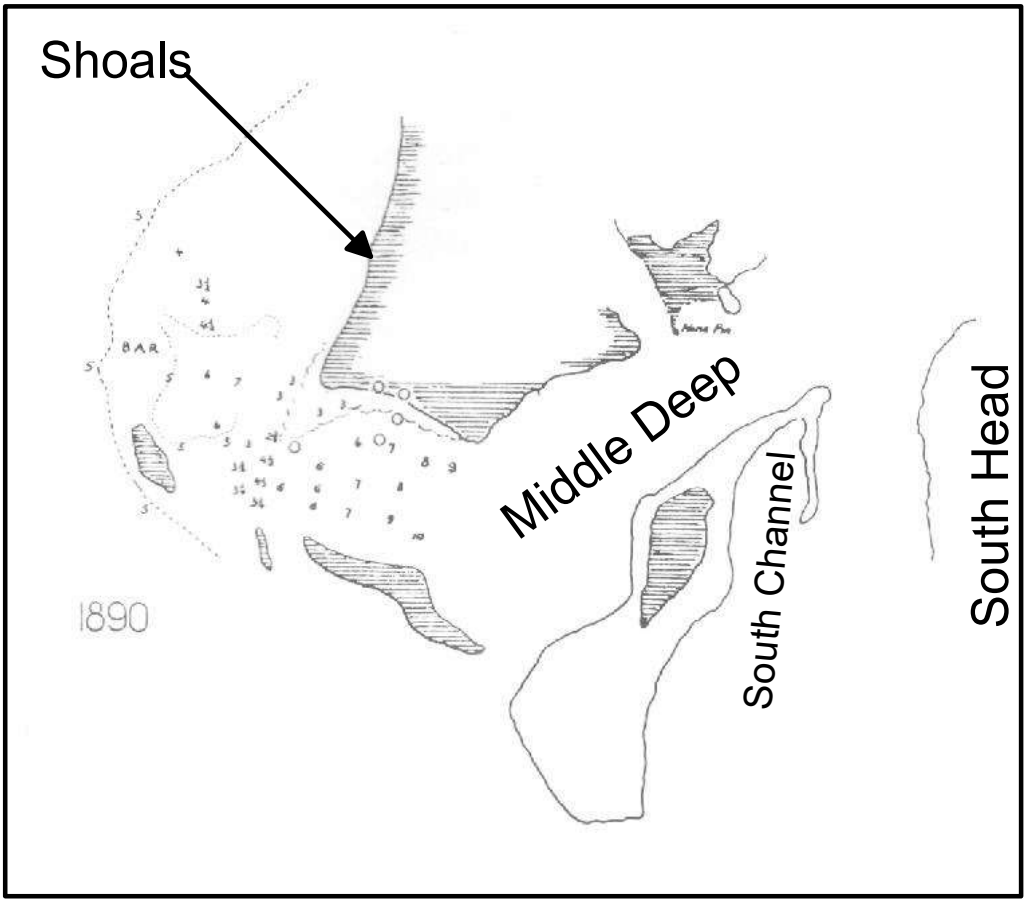
Shoals
Middle Deep
South Channel
South Head
1890

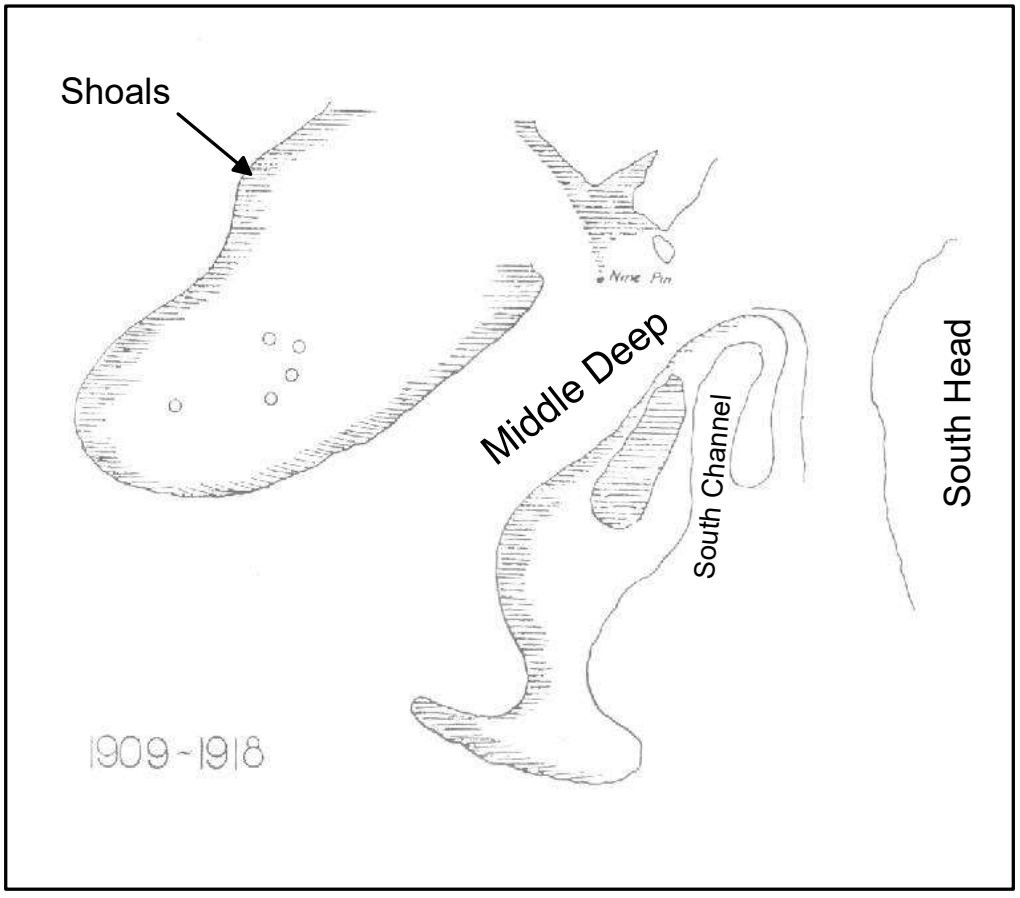
Shoals
Middle Deep
South Channel
South Head
1909-1918

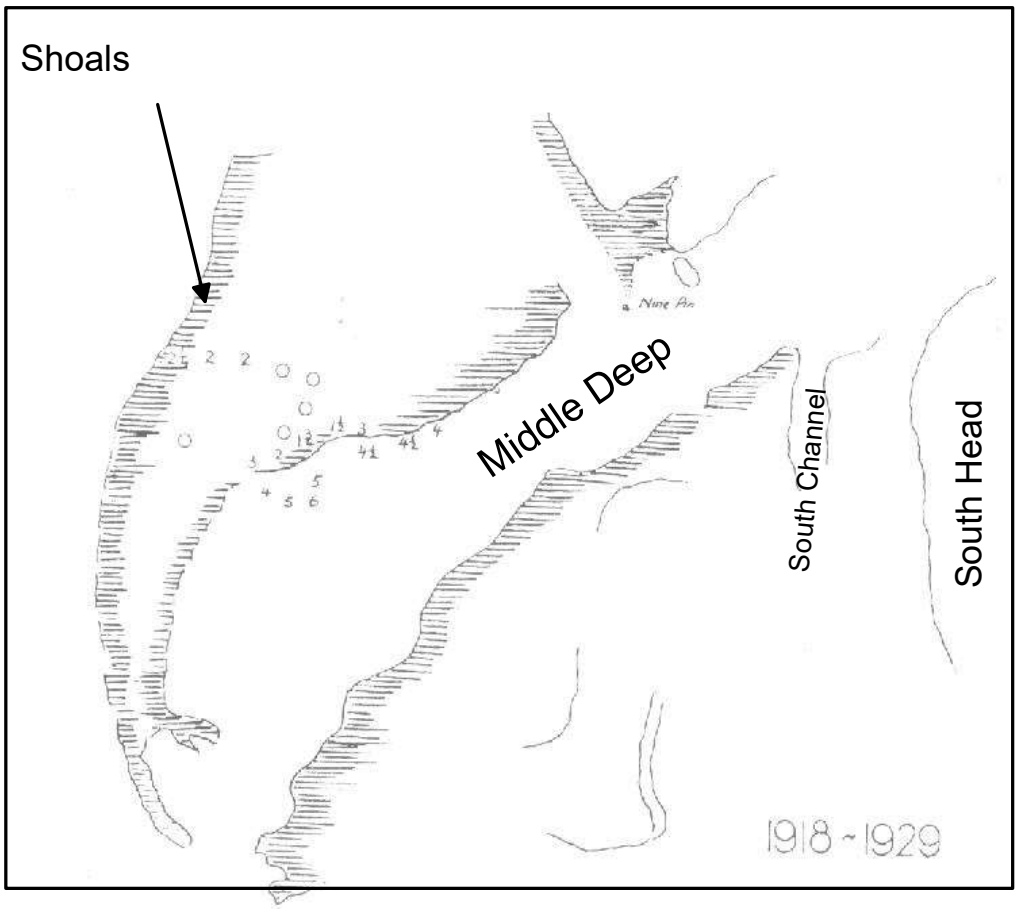
Shoals
Middle Deep
South Channel
South Head
1918 - 1929

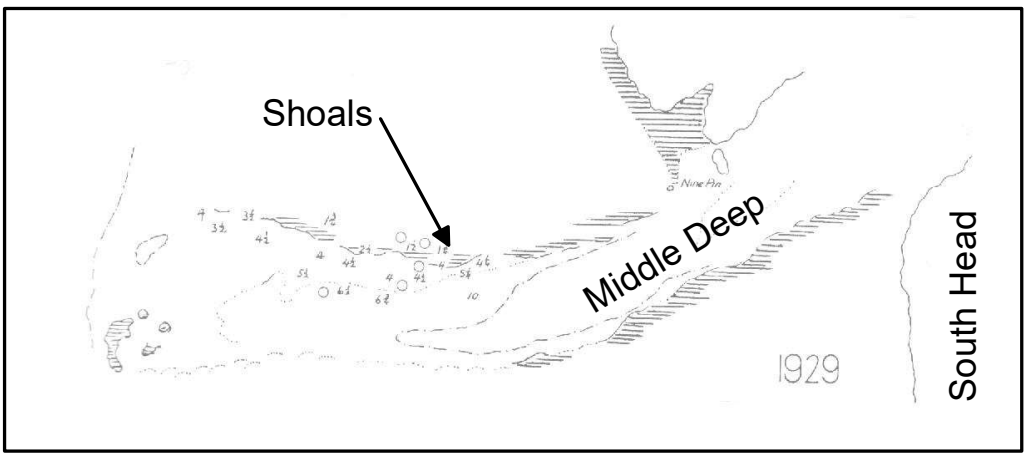
Shoals
Middle Deep
South Head
1929

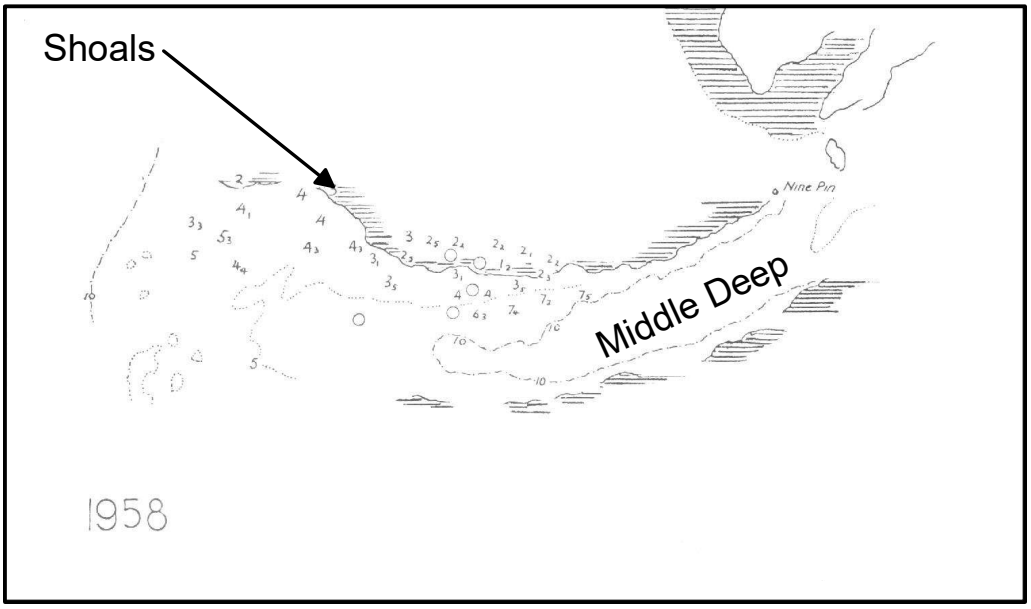

Figure 1.8. Changes in the orientation of the ebb tidal delta and terminal lobe at the entrance to Manukau Harbour; 1864 to 1958 (Fairburn, 1987).

Satellite imagery of the Manukau ebb tidal delta covering the 4-year period from December 2013 to September 2017 (Figure 1.9) shows the evolution of the shoals and the orientation of the ebb jet at monthly/seasonal and annual time scales; 26 images are available for this period. The ebb jet is angled distinctly to the west oceanward of the Manukau Heads during this period and appears to split in half from around March 2016, when a more southward orientated channel breaches the terminal lobe. This split ebb channel persists and is clearly evident in the June 2017 image, which illustrates the formation of the “batwing shaped” delta terminus.

2013-12-14-22-13-45 L8

2014-01-31-22-13-16 L8

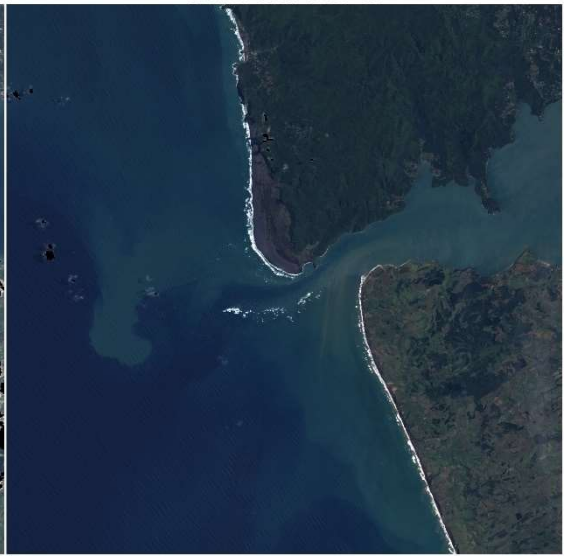

2014-03-20-22-12-37 L8

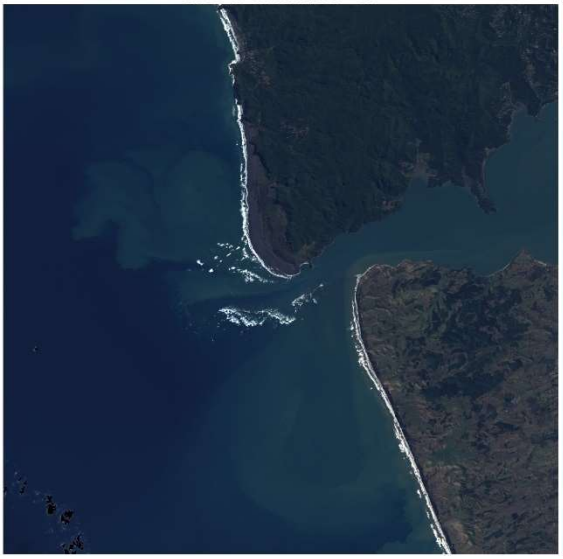

2014-04-30-22-05-46 L8

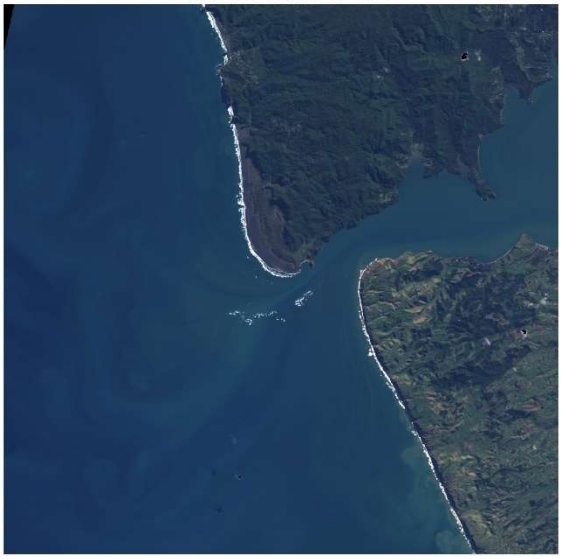

2014-05-07-22-11-50 L8

2014-12-01-22-12-24 L8

2015-02-28-22-05-48 L8

2015-08-07-22-05-40 L8

2016-03-02-22-05-55 L8

2016-08-16-22-12-17 L8

2016-09-10-22-06-15 L8

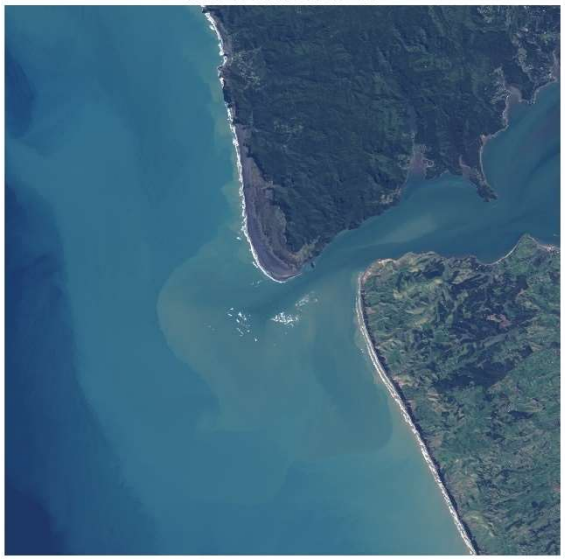

2016-10-28-22-06-23 L8

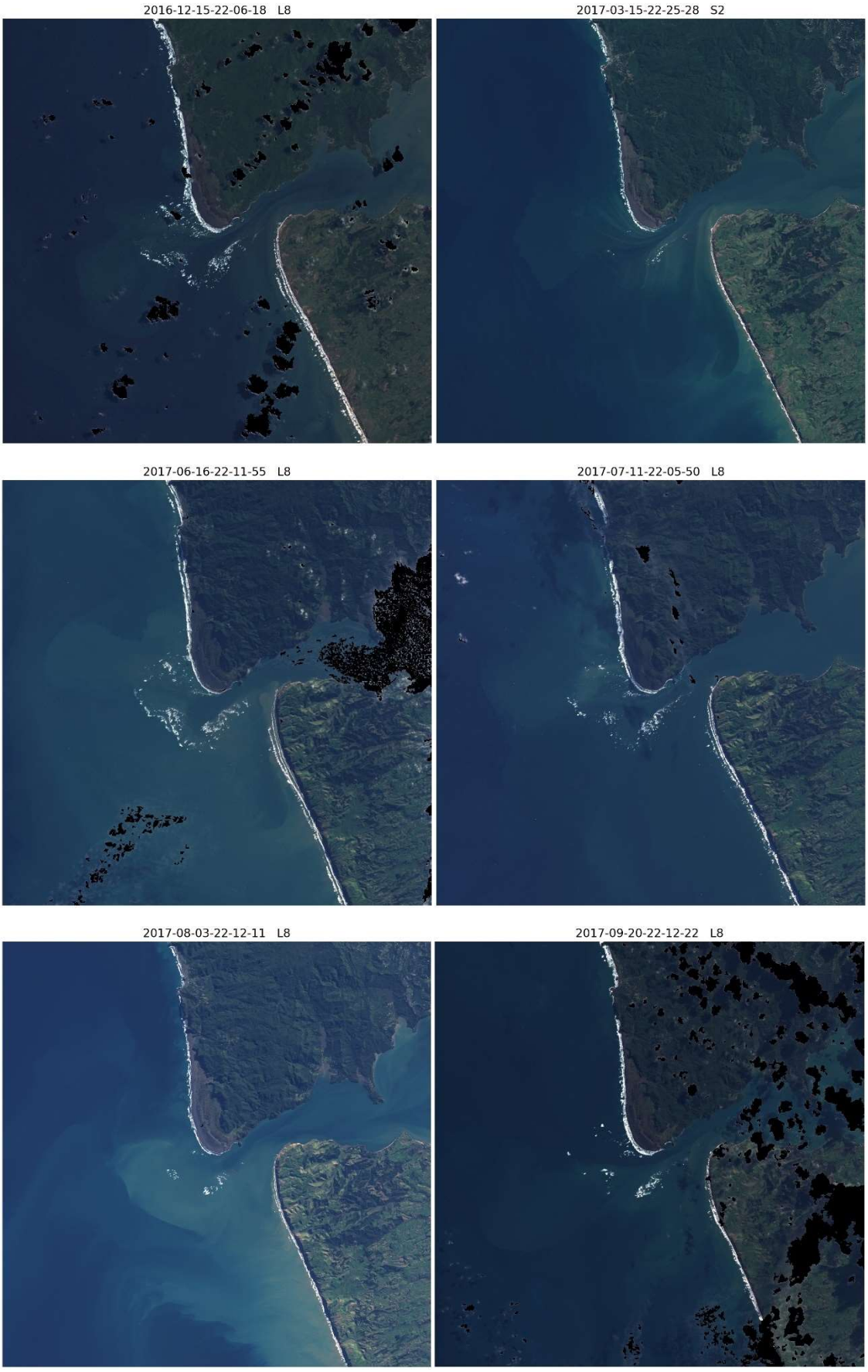

Figure 1.9. Satellite imagery of the Manukau ebb tidal delta covering the period Dec 2013 – Sep 2017.

2 Review of Similar Studies

Modelling studies of dredge channel infilling and volumes dredged from dredged entrance channels were reviewed to provide further insight into annual maintenance dredging in the present case, as well as to support the interpretation of the numerical modelling of Manukua Heads.

Fernández-Fernández *et al.* (2019) undertook a modelling assessment of the lifetime of various dredging scenarios at the entrance to the Figueira da Foz tidal inlet, on the open coast of western Portugal. Under high-energy wave conditions, which can be considered analogous to the typical wave environment at Manukau, the largest dredge volume of the study of 2,925,000 m^3 was completely infilled after 60 days. The tidal prism of the Figueira da Foz estuary is substantially smaller than that of the Manukau (890,000 m^3 compared to 918,000,000 m^3), however, both systems are bypassed by considerable volumes of longshore wave driven sediments each year, with Figueira da Foz more than doubling Manukau, having an estimated transport rate of 1,000,000 m^3/year (Fernández-Fernández *et al.*, 2019) as opposed to 375,000 m^3/year (Mead *et al*., 2010). With exposure to consistent high-energy wave conditions and a substantial littoral drift system, this study provides some insight for likely maintenance dredging requirements at Manukau, although the tidal prism (which drives currents through the entrance) is greatly reduced (by 3 orders of magnitude) and significantly greater alongshore sediment transport rates are distinctly different features at Figueira da Foz.

Pion and Bernadino (2018) modelled maintenance dredging volumes in the entrance to the Port of Santos, Brazil. While the wave climate here is less energetic than the Auckland west coast, wave heights periodically exceed 5 m in the winter months. In order to maintain approach channel depths of 12.6 m, it was found that 1,644,000 m^3/year of material would require dredging. The Port of Santos on the Brazilian east coast has a more moderate wave climate in comparison to the Auckland west coast.

Reyes-Merlo *et al.* (2017) analysed the efficiency of historical dredge operations at the Punta Umbría tidal inlet in south-western Spain. The entrance to the estuary experiences average wave heights of between 0.5 – 1.0 m, which is a considerably less energetic wave environment than that of the Manukau Harbour, however, spring tidal ranges are comparable between the two systems (Table 2.1) as well as the volume of sediment supplied via longshore drift (300,000 m^3/year at Punta Umbría). The period 2004 – 2014 required an average of 44,000 m^3/year of material to be removed to maintain the navigability of the entrance channel.

Although Port Taranaki in New Plymouth, New Zealand, is relatively sheltered in comparison to Manukau Harbour, due to its orientation to the predominant swell direction, there is a high potential for sediment transport from the west to the east. Port Taranaki Ltd dredged

1,300,000 m^3 of material from the entrance channel between 1989 and 1998, some 145,000 m^3/year (McComb and Black, 2000). While McComb (2001) calculated that sediment transport in the area was approximately 220,000 m^3/year. Similarly, at Port Otago some 500,000 m^3/year of gross sediment transport has been previously calculated, although around 200,000 – 250,000 m^3 of entrance channel dredging will be required each year to maintain the 14 m deep entrance channel (P. McComb, pers. comm.). Thus, less material than that transported across the channel likely requires dredging. A similar scenario is found for the Port of Tauranga maintenance dredging of the entrance channel through the ebb tidal delta; gross sediment transport has been calculated at 210,000 m^3/year (Mead and Black, 1999), while average annual dredge volumes are 74,000 m^3/year.

Table 2.1 below provides a comparison between Manukau and other harbours in New Zealand and overseas in terms of their tidal prism, tidal range, wave climate and entrance channel annual dredge volumes. From these data, there is some indication that higher alongshore sediment transport rates result in higher annual dredge volumes, noting this is based on net alongshore sediment transport (Figure 2.1). It is notable that the Auckland west coast does not have a particular large alongshore sediment rate; this is due to the orientation of the coast being almost shore-normal to dominant incident waves from the southwest.

Table 2.1. Tidal prism, tidal range, wave climate and entrance channel annual dredge volumes for a range of tidal inlets in New Zealand and overseas (Bell *et al*., 1998; Fernández-Fernández *et al*., 2019; Pion and Bernadino, 2018; Castelle *et al*., 2007; McComb and Black, 2000; McComb, 2001; Ramli *et al*., 2015; Trombetta *et al*., 2019; Mead and Black, 1999).

	Spring Tidal Prism (m^3)	**Spring Tidal Range (m)**	**Wave Climate**	**Dredge Volume (m^3/year)**	**Alongshore Drift Volume (m^3/year)**
Manukau Harbour	918,000,000	3.4	Highly Energetic	-	225,000 375,000*
Figueira da Foz (Portugal)	890,000	2.2	Highly Energetic	>2,925,000[M]	1,000,000
Port of Santos (Brazil)	55,100,000	1.2	Moderately Energetic	1,644,000[M]	355,000
Punta Umbría (Spain)	20,000,000	3.2	Weakly to Moderately Energetic	44,000 [D]	300,000
Currumbin Creek (Australia)	1,610	1.5	Moderately to Highly Energetic	46,000 [D]	500,000 800,000*

Port Taranaki	-	3.2	Moderately Energetic	145,000 [D]	220,000
Port of Otago	69,000,000	2.15	Moderately Energetic	250,000[D]	500,000
Port of Tauranga	178,000,000	1.6	Moderately Energetic	62,000 [D]	73,000 210,000*

[M] denotes modelled volume

[D] denotes dredged volume

* Denotes combined value of the up-coast and down-coast longshore drift volumes; gross as opposed to the net sediment transport value.

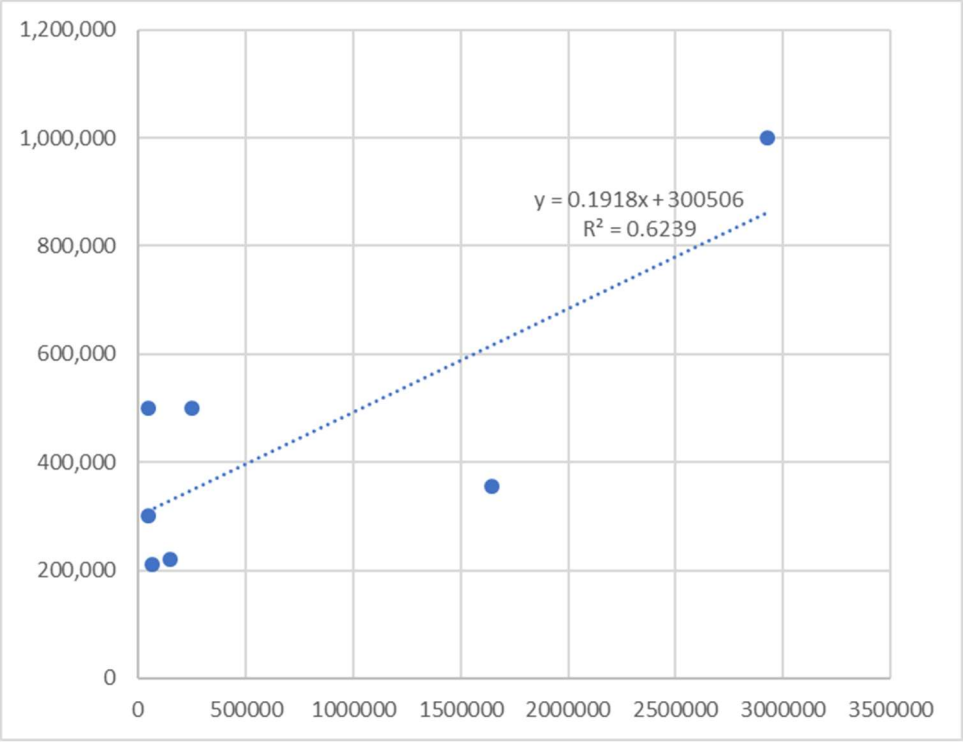

Figure 2.1. Net alongshore sediment transport rates versus annual dredge volumes from Table 2.1

3 Numerical Modelling

Two-dimensional hydrodynamic and wave models were employed to provide an initial insight into potential infilling of a dredged entrance channel through the Manukau Harbour ebb-tidal delta. The hydrodynamic model used was D-Flow Flexible Mesh (D-Flow FM), which covered the outer and inner harbour, while the wave model used was SWAN, which covered just the outer harbour where the wave climate is relevant. The hydrodynamic model is described in 3.2 and the wave model is described in 3.3. Both models were run for six individual historical scenarios, which were selected in order to give a representative range of energy environments (see 3.1 for scenario details). Each scenario was simulated using both current (non-dredged) and digitised dredged bathymetry for comparison. Model results from D-Flow FM and SWAN were analysed independently and then combined in order to determine their net effect (3.4). As noted in Section 1, this modelling is uncalibrated, as no site-specific data are available for the Manukau Heads in terms of sediment properties, waves/currents and bathymetry. Simple calibration using the Paratutae Island and Onehunga tide gauges was undertaken (Section 3.3.3).

3.1 Modelled Scenarios

Three separate years were modelled on both the non-dredged and dredged bathymetries to capture the range of energetics experienced on the Manukau ebb tidal delta – high energy, low energy and average energy. These years were chosen following the methods of Fernández-Fernández *et al*. (2019) where the deep-water wave power energy (P) was derived for every entry in the long-term offshore wave record according to:

$$P = 0.49\, H_s^2\, T_e \qquad (1)$$

Where H_s is the significant wave height and T_e is the wave energy period which can be estimated from the zero-crossing period (T_{02}) as in Cahill and Lewis (2014):

$$T_e = 1.32\, T_{02} \qquad (2)$$

P was averaged over each year and the high, low and average years were determined to be 1991, 2017 and 2010 respectively based on wave data sourced from the ECMWF (European Centre for Medium-range Weather Forecasts) wave hindcast (ERA-5).

Additionally, three large individual wave events were simulated over both the non-dredged and dredged bathymetries (Table 3.1). These were selected from the long-term offshore wave record based on their extremity and direction and include the largest recorded event (17-Apr-

1999 from the southwest[2]), as well as the largest west swell (14-Jun-1993) and northwest swell (11-Jul-1986).

Table 3.1. Extreme events in the offshore wave record.

Event	H_s (m)	T_p (s)	D_p (degrees)
17-Apr-1999	10.5	15.4	235
14-Jun-1993	9.3	14.9	252
11-Jul-1986	7.8	13.5	285

3.1.1 Model Assumptions and Limitations

Several assumptions have been made for the numerical modelling, some of which may not be valid, although these are unknowns in the absence of site-specific field data:

- Assume that the bar is non-consolidated sediment in calculations;
- No wave calibration data are available, however, experience using SWAN indicates that it performs relatively well on open coasts when non-calibrated;
- Limited sea level calibration data (only high and low tide times) was used to calibrate water levels;
- Current speeds are based on single-value current data from existing reports;
- Assumed a uniform bottom friction;
- Non-coupled modelling of waves and currents, which were evaluated through the combination of model outputs;
- The dredge channel was 15.5 m deep, 250 m wide at the bottom with 1:4 slopes on either side (this may be different with detailed design):
- Assumed values for d_{50} and d_{90} grain sizes, bed slope β, roughness length z_0 and other calculation parameters based on existing information for the west coast and Manukau Harbour;
- Long-term morphological changes to the ebb-tidal delta have not been considered, and;
- The focus is on the entrance through the Manukau Bar; dredge requirements for the inside of the harbour have not been assessed, although are expected to be significantly lower than the entrance channel, noting that much of the natural channel system within the harbour is already deeper than 15.5 m.

[2] This event has been estimated to be a 1 in 1,165 year return period event (Mead, 2006).

3.2 Hydrodynamic Modelling

The hydrodynamic modelling software used for this project is D-Flow Flexible Mesh (D-Flow FM) by Deltares, part of the Delft3D FM Suite (Deltares, 2019). D-Flow FM simulates two or three-dimensional unsteady flow by solving the horizontal equations of motion, the continuity equation and the transport equations for conservative constituents. D-Flow FM works with unstructured grids, meaning model cells can be from 3-sided up to 6-sided and irregularly shaped. This grid format allows model cell shape and size to be manipulated based on the morphology of areas of interest, negating the need for multiple model domains and making simulations more accurate and efficient, which was very useful for developing the model domain for inside the Manukau Harbour.

3.2.1 Bathymetry Grid

Bathymetry for the model grid was sourced from the digitised hydrographic chart NZ4314 of Manukau Harbour, as well as a manual digitisation of the proposed dredged channel for corresponding dredge channel scenarios. Bathymetry was interpolated onto the model grid using a scattered interpolant. Figure 3.1 and Figure 3.2 show the grid and bathymetry for the outer and inner harbour, respectively.

The digitised dredge channel was 15.5 m deep, 250 m wide at the bottom with 1:4 slopes on either side; as considered for the Future Ports Study (2016). The channel was designed to run through the ebb-tidal delta, following the Entrance Channel, then Papakura Channel of the Manukau Harbour to terminate at Pukenui (Figure 1.3 for channel names, Figure 3.3 for proposed channel). Because much of the natural channel system within the harbour is already deeper than 15.5 m, the dredge channel was only digitised in the zones that were shallower than this, which were the ebb-tidal delta (Figure 3.4) and the Papakura Channel approaching Pukenui (Figure 3.5).

At the open ocean, model cells were large nested squares, with their main purpose to propagate the tidal boundary condition into the harbour (Figure 3.1). Within the harbour, the channel cells were designed as elongated rectangles, designed to efficiently guide flow through the channels (Figure 3.2). Intertidal areas, where flow is not channelized, were filled with triangular cells. Model cell sizes varied depending on the areas of interest, with the boundary cells approximately 7000 m by 7000 m and channel/intertidal cells as small as 100 m by 100 m.

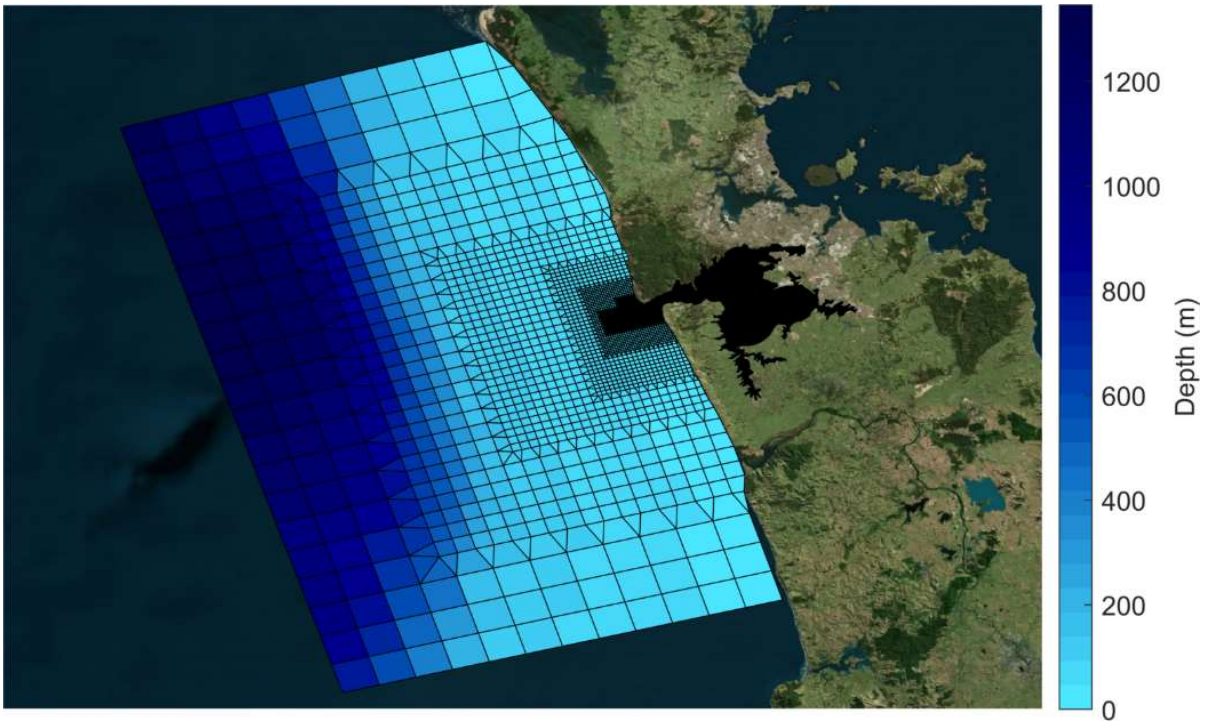

Figure 3.1. Grid and bathymetry for the Manukau Harbour hydrodynamic model.

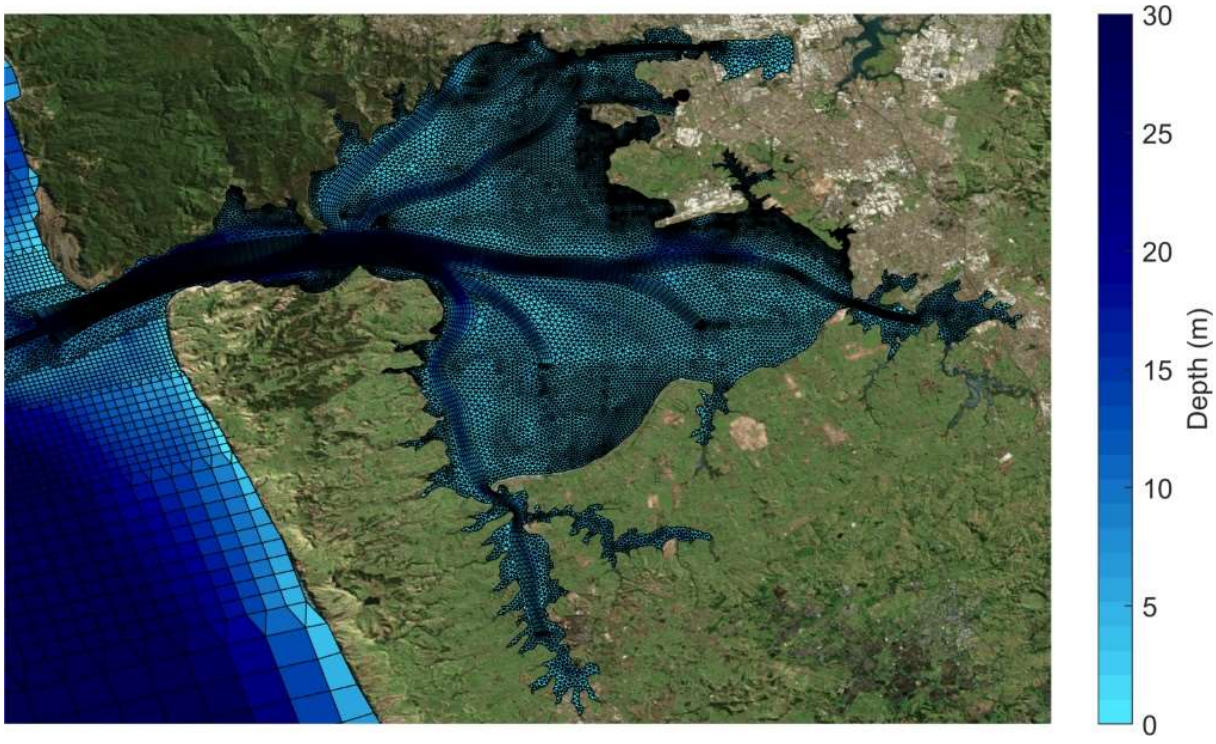

Figure 3.2. Magnified view of the grid and for the hydrodynamic model, showing the elongated grid cells in the harbour channels and triangular cells in intertidal areas.

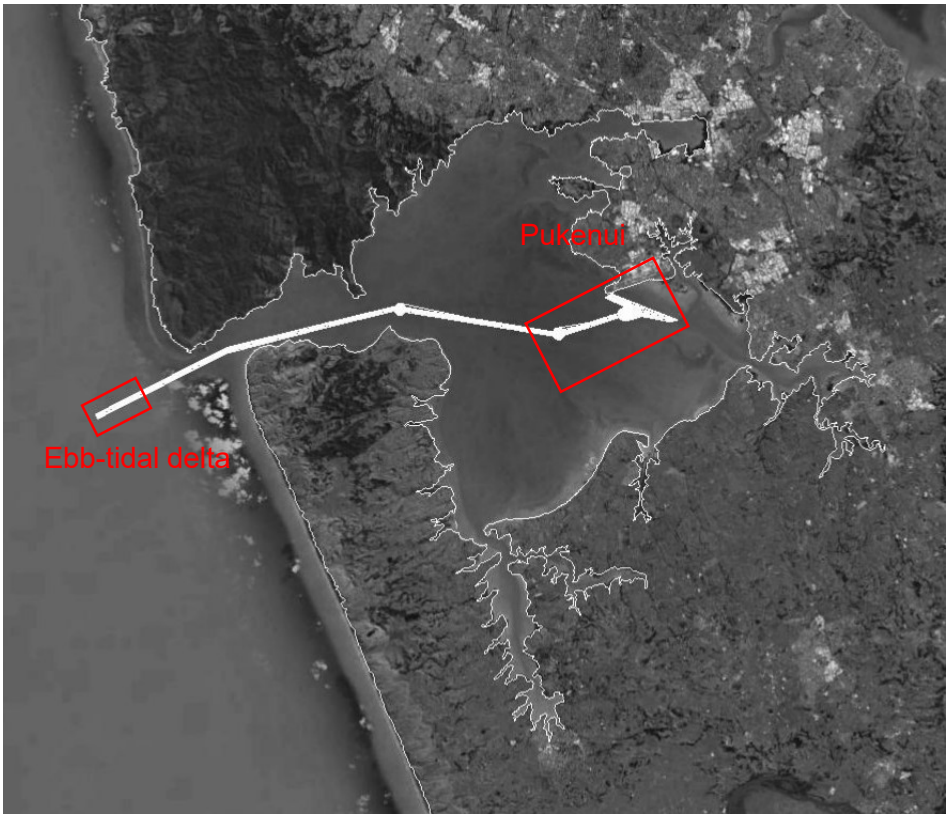

Figure 3.3. Design of the proposed channel through the Manukau harbour. Red squares indicate sections of the proposed channel that are currently shallower than 15.5 m and will need capital dredging.

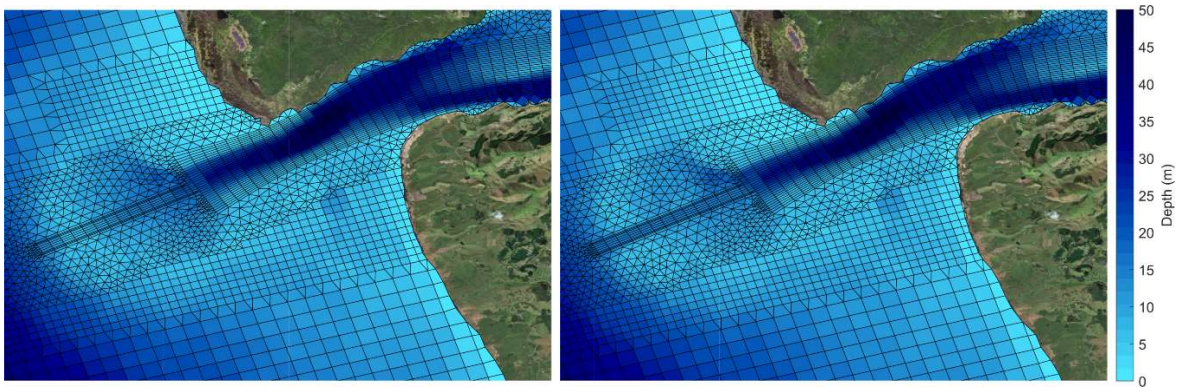

Figure 3.4. Grid and bathymetry for the hydrodynamic model showing the ebb-tidal delta bathymetry for the original (left) and dredged (right) scenarios. Note the only difference between the bathymetries is the deeper channel through the ebb-tidal delta (right, see Figure 3.3 for dredged areas).

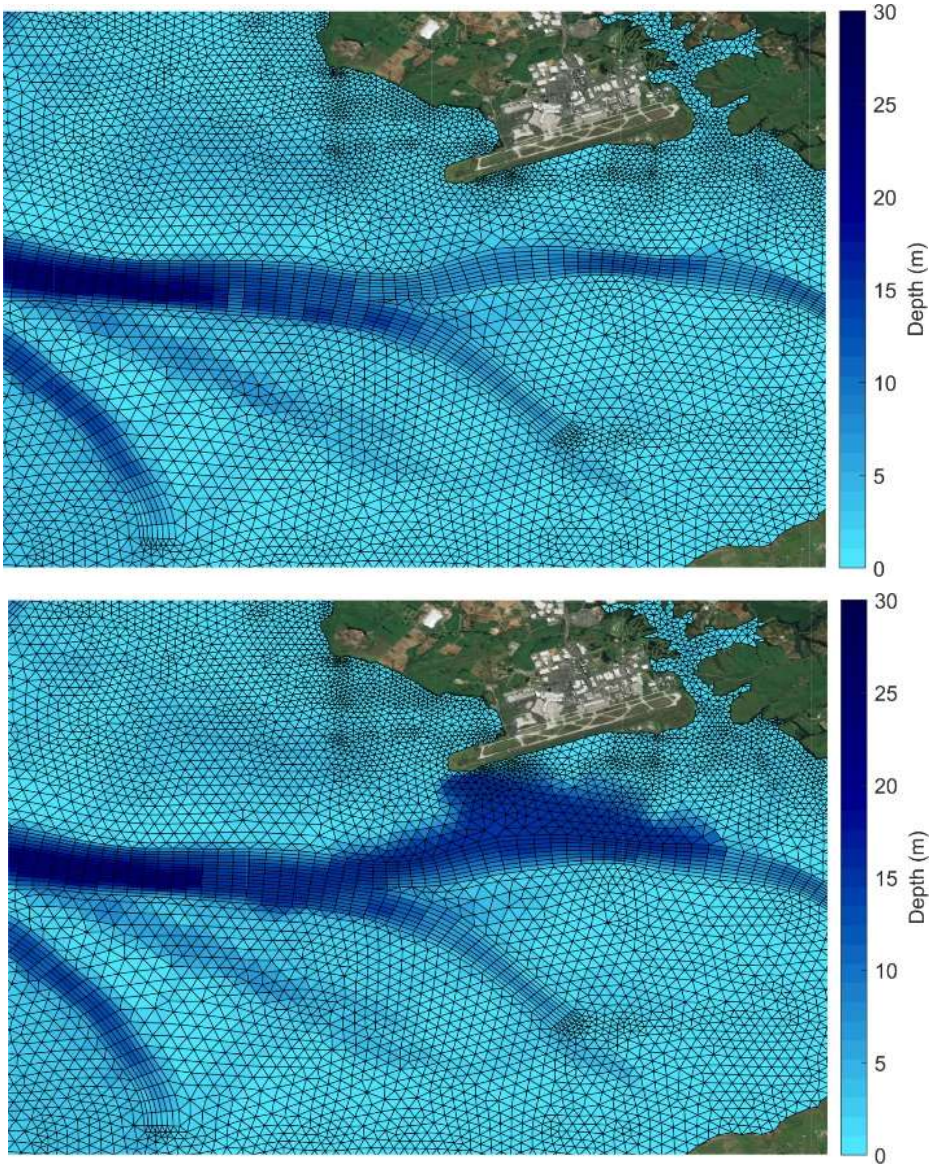

Figure 3.5. Grid and bathymetry for the hydrodynamic model showing the bathymetry at Pukenui as it currently exists (top) and dredged (bottom) scenarios.

3.2.2 Boundary Conditions

Tidal boundary conditions on the open ocean boundaries of the model were extracted from the TPXO wave atlas (Egbert and Erofeeva, 2002). This model was developed by the Oregon State University, who created a global model of ocean tides which uses along track averaged altimeter data from the TOPEX/Poseidon and Jason satellites since 2002. The methodology applied in the global tide models has been refined to create higher resolution regional models. For this project, the Pacific Ocean model with a resolution of 1/12 degree was utilised. The model provided the 11 most influential constituents, as well as two long period (Mf, Mm) harmonic constituents. Each constituent is a sinusoid which represents the gravitational influence of a particular aspect of a planetary body or of several bodies. Each sinusoid was

described in the model by a phase and amplitude of the sinusoid and these were extracted at regular intervals along the model boundary.

10 m elevation wind and pressure at mean sea level were extracted from the NCEP Climate Forecast System (Kalnay *et al.*, 1996), which has a grid resolution of 1/5 degree. These were used to create a spatially and temporally varying wind and pressure conditions that covered the entire model domain.

3.2.3 Model Calibration and Sensitivity Testing

Although the scope of the project did not include calibrating the hydrodynamic model, a simple model calibration/validation was undertaken using high and low tide water levels at the Paratutae Island and Onehunga tide gauges (Figure 3.6). Figure 3.7 shows that model water levels agreed with the measured data at the Paratutae Island tide gauge in the Entrance Channel of the Manukau Harbour. The model also captured high tide levels at the Onehunga tide gauge in the upper reaches of the harbour, but failed to reach low tide levels on spring tides (Figure 3.7). A variable friction map in the model would likely improve the water level calibration at the Onehunga tide gauge, but would require an in-depth field survey of the Manukau Harbour in order for sensible values to be selected.

The two model physical parameters that were sensitivity tested were the horizontal eddy viscosity and the uniform bottom friction. For the eddy viscosity, the Smaogrinsky horizontal model was used, which is designed to cope with large variations in grid cell sizes as we see in the Manukau Harbour model. Typical values for the Smagorinksy coefficient are between 0.1 and 0.2 (Rösler, 2015), so these values were used as our range for sensitivity testing. Model results were found to be generally insensitive to Smagorinsky coefficient settings so a value of 0.15 was used. Conversely, model water levels and currents were notably sensitive to changes in bottom friction. Manning's n values between 0.015 and 0.04 were tested, based on Chow's (1959) lower and upper limits for excavated or dredged channels. A final value of 0.018 was used, which balanced accuracy of water levels at the Entrance Channel (Figure 3.7) and current speeds in the Entrance Channel, which are expected to reach approximately 2.25 m/s on a typical spring ebb tide (Heath *et al*., 1977).

Figure 3.6. Locations of tide gauges used for basic model calibration.

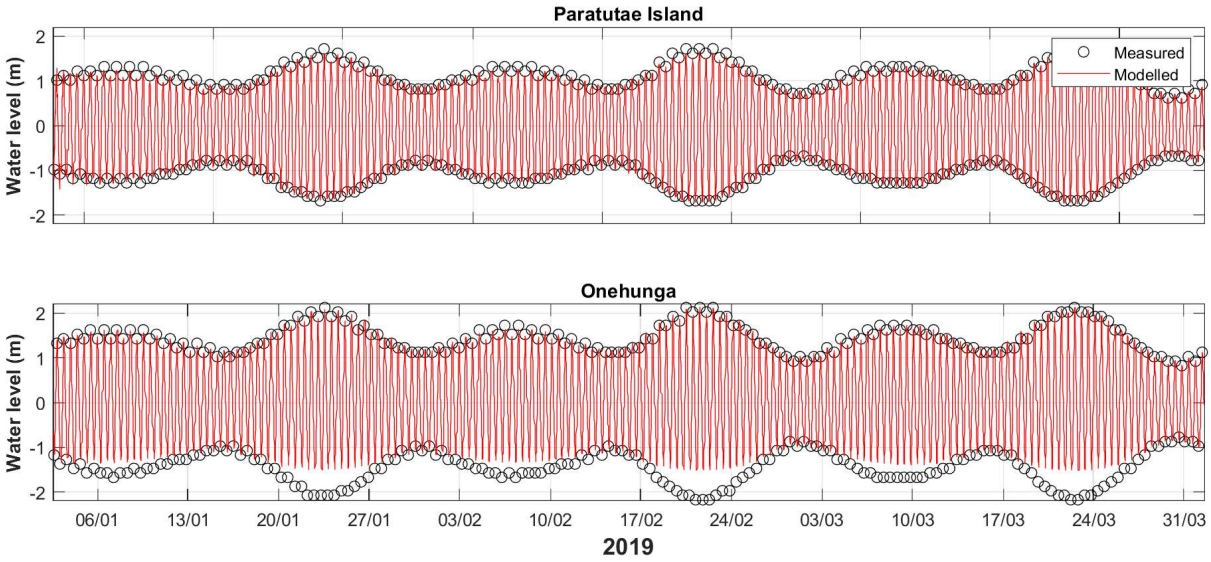

Figure 3.7. Water level calibration of the hydrodynamic model at two locations within the Manukau Harbour over the period 1 January 2019 to 1 April 2019. Modelled water levels were calibrated to high and low tide measurements at the Paratutae Island and Onehunga tide gauges.

3.3 Wave Modelling

Wave transformation was undertaken using the wave model SWAN (Simulating WAves Nearshore) which is part of the Delft3D model suite. SWAN is a third-generation ocean wave propagation model, incorporating current knowledge regarding the generation, propagation

and transformation of wave fields in both deep water and nearshore regions. SWAN solves the spectral action density balance equation for frequency-directional spectra. This means that the growth, refraction, and decay of each component of the complete sea state, each with a specific frequency and direction, is solved, giving a complete and realistic description of the wave field as it changes in time and space. Physical processes that are simulated include the generation of waves by the surface wind stress, dissipation by white-capping, resonant nonlinear interaction between the wave components, bottom friction and depth limited breaking. The model is described by Holthuijsen *et al.,* (2004).

Hindcasted global wave models provide long term wave conditions worldwide. These models, however, are run over a coarse bathymetry and consequently do not account for the effect of local features on the wave climate in shallow water locations. To account for this, we used a nested modelling methodology to refine results from the global wave model. Nesting involves running a model over a large area and using the results from this to provide boundary conditions for a model covering a smaller region at a higher resolution. This process is repeated until a suitable resolution is achieved over the area of interest.

3.3.1 Wave-Current Interaction

To get an initial overview of how constructing a dredge channel through the Manukau Harbour ebb-tidal delta might affect sediment dynamics, shear stresses were produced from the results of the hydrodynamic model and the wave model combined. Tidal current and wave shear stresses were combined using the following equations from Soulsby (1997):

$$\tau_m = \tau_c \left[1 + 1.2 \left(\frac{\tau_w}{\tau_{c+}\tau_w}\right)^{3.2}\right] \quad (3)$$

$$\tau_{max} = [(\tau_m + \tau_w cos\varphi)^2 + (\tau_w sin\varphi)^2]^{1/2} \quad (4)$$

Where τ_m is the mean combined shear stress, τ_c is the shear stress due to currents alone, τ_c is the shear stress due to waves alone, τ_{max} is the maximum combined shear stress and φ is the direction of shear stress.

Figure 3.8 shows the mean shear stress for the year-long model simulations for both the original (non-dredged) and dredged bathymetries. As with wave heights (Figure 3.20), there was very little difference in mean shear stress between the years. Tidal currents are not expected to differ greatly on an annual basis, it is therefore not surprising that mean annual shear stress depends heavily on the annual wave characteristics. The greatest shear stresses were found on the southern side of the Entrance Channel rather than on the ebb-tidal delta. Figure 3.9 illustrates the difference between the original and dredged bathymetries for the

year-long model simulations. The construction of the dredge channel decreases the shear stress within the proposed channel and increases shear stress on the ebb-tidal delta surrounding the proposed channel. This indicates that the shear stresses in the outer Manukau Harbour depend mostly on waves, as wave heights decreased at the proposed channel in dredged simulations, but tidal currents increased. Furthermore, wave heights slightly increased on the ebb-tidal delta surrounding the proposed channel while tidal currents decreased.

There was a greater difference between shear stresses in the month-long extreme event simulation (Figure 3.10). July 1986, being the smallest event (Table 3.1), produced noticeably lower shear stresses than the other two events. Interestingly the June 1993 event produced larger shear stresses than the more extreme April 1999 event. This is because wave direction is an important factor in the generation of shear stress on the ebb-tidal delta, and that a direct westerly swell can cause greater shear stress than a larger south-westerly swell due to the orientation of the coast and the bar (as described in Section 2 above). Despite the shear stresses for each event varying, the differences in shear stresses between original and dredged scenarios were similar (Figure 3.11).

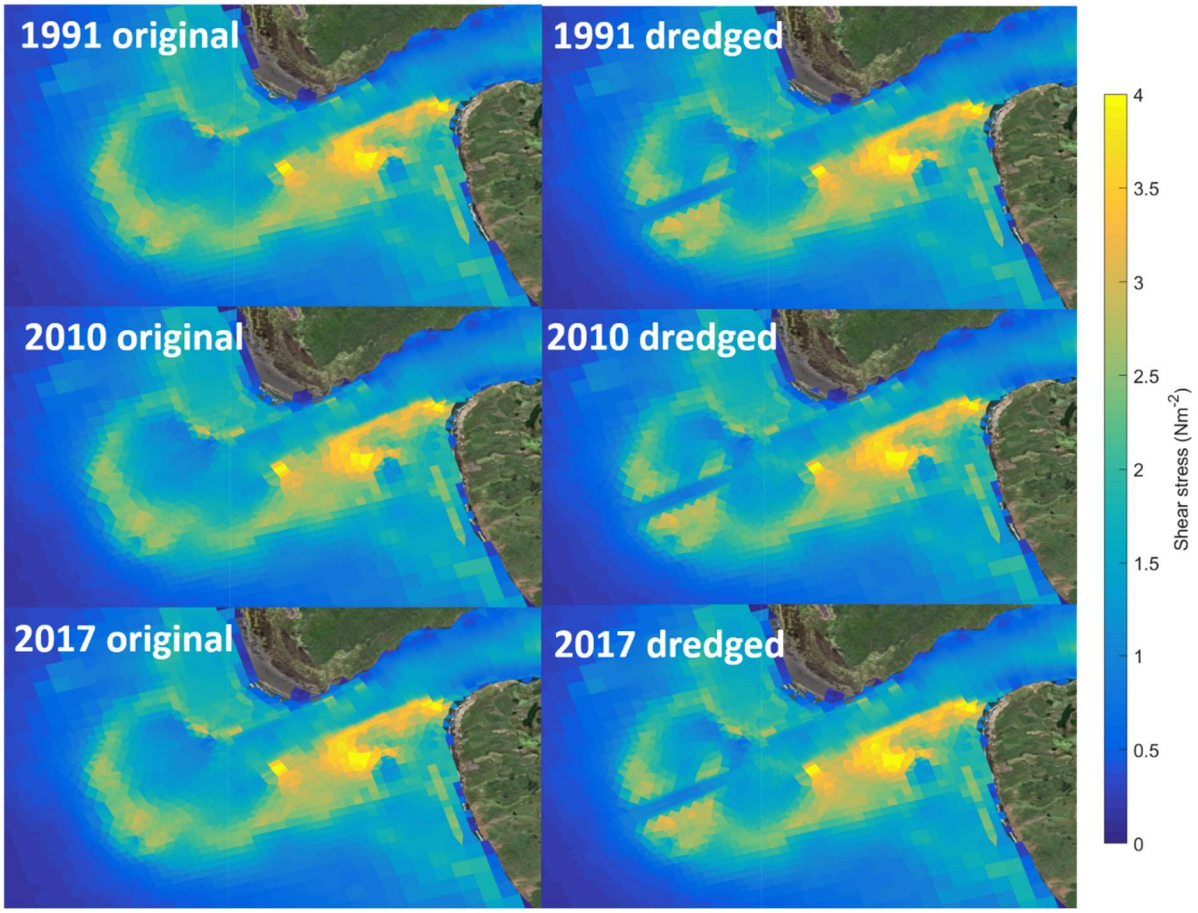

Figure 3.8. Mean shear stress for dredged and original bathymetry for the year-long model runs.

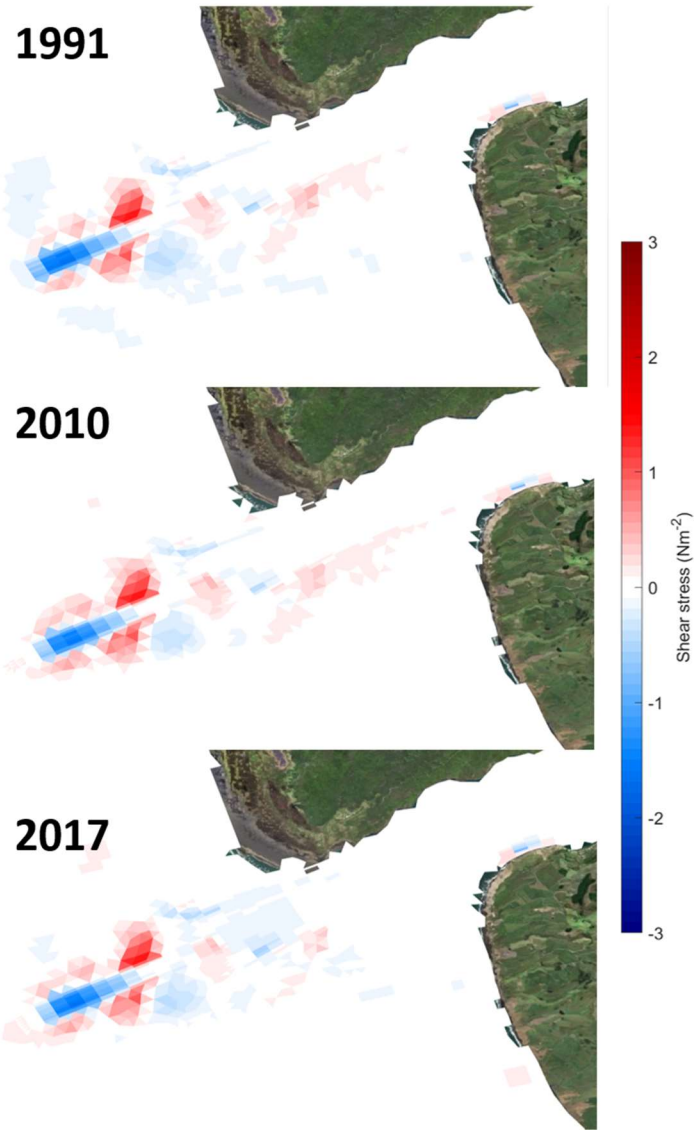

Figure 3.9. Difference in mean shear stress between dredged and original bathymetry for the year-long model runs. Positive numbers indicate higher shear stress in the dredged scenario.

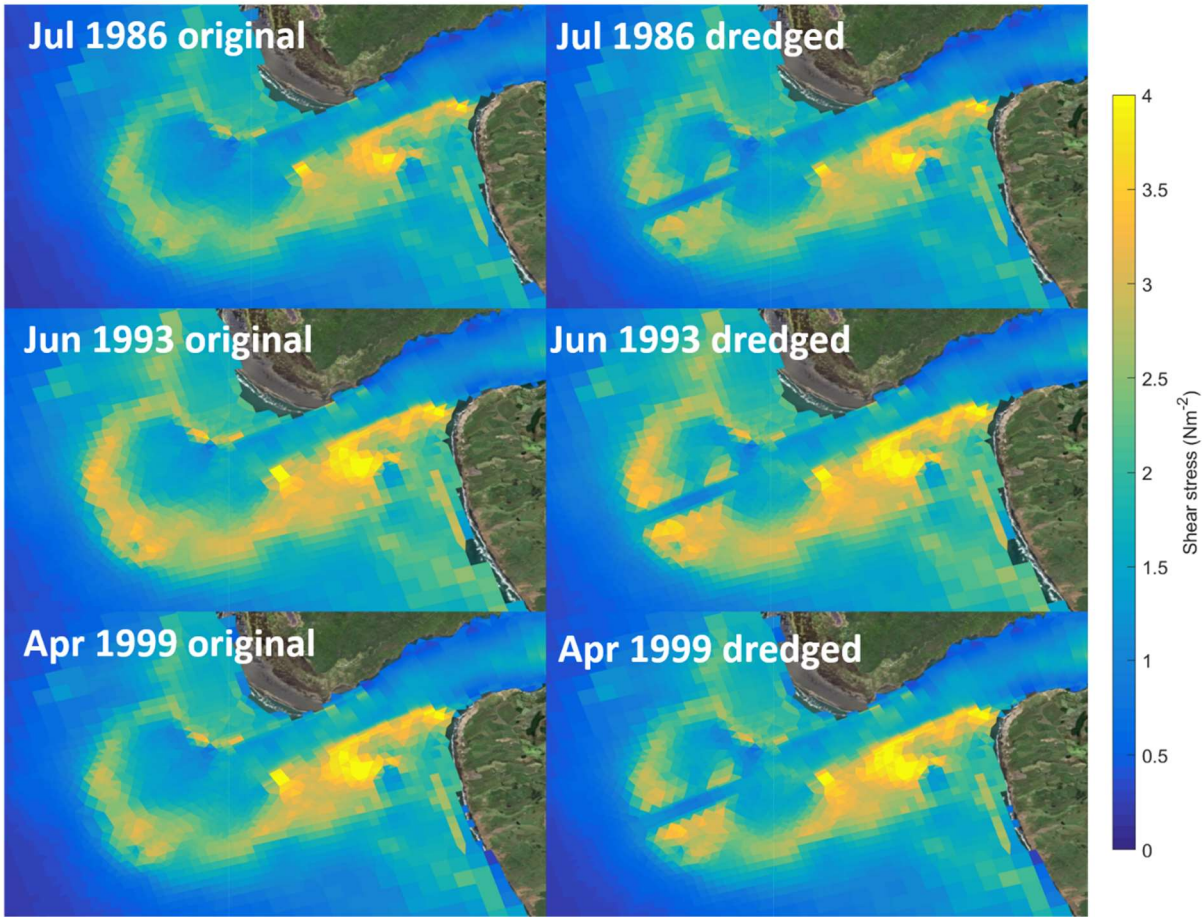

Figure 3.10. Mean shear stress for dredged and original bathymetry for the extreme conditions listed in Table 3.1.

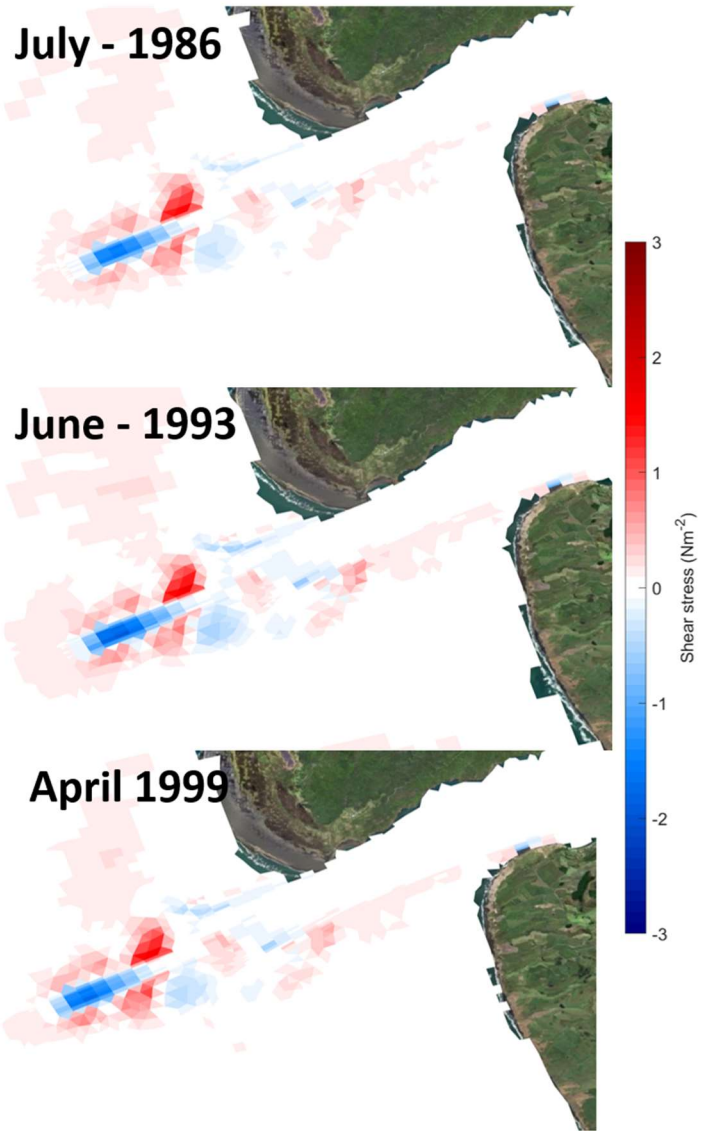

Figure 3.11. Difference in mean shear stress between dredged and original bathymetry for the extreme conditions listed in Table 3.1. Positive numbers indicate higher shear stress in the dredged scenario.

3.3.2 Bathymetry Grid

The first stage in this process involves the creation of a series of bathymetric grids for each nested region of the outer Manukau Harbour. Bathymetry data was taken from the digitised hydrographic chart NZ4314 of Manukau Harbour and the NIWA 250 m national gridded bathymetry dataset (NIWA, 2016). These data were combined and used to interpolate the depths over regularly spaced grids using a kriging gridding methodology. The 3 grids generated by this process are shown in Figure 3.12. The inner grids have a horizontal resolution of approximately 55 x 55 m.

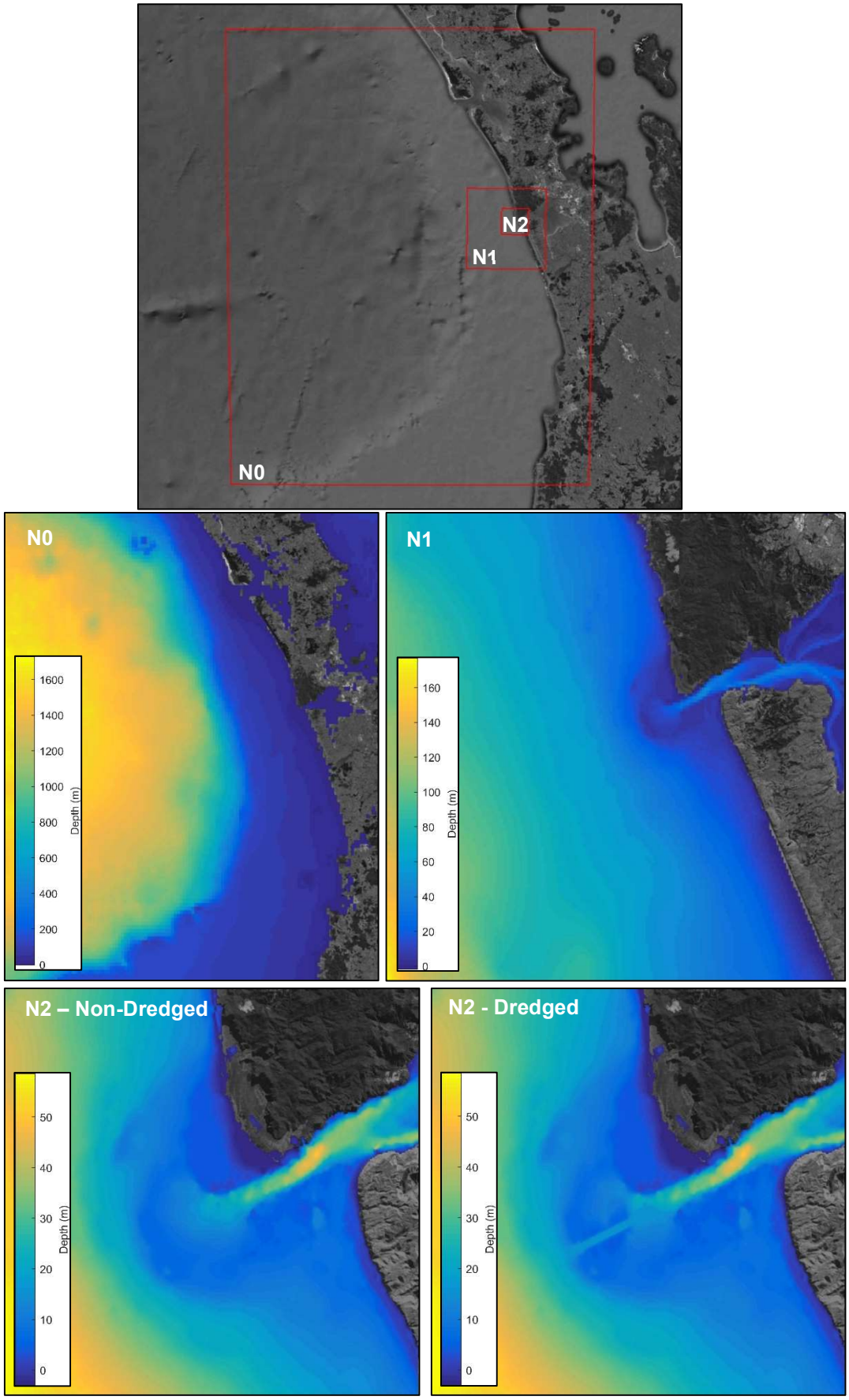

Figure 3.12. SWAN model grids. Red boxes indicate the spatial extent of the nests and the colour plots illustrate the bathymetry of the N0, N1 and N2 non-dredged and dredged domains

3.3.3 Boundary Conditions

Boundary conditions were sourced from the ECMWF (European Centre for Medium-range Weather Forecasts) wave hindcast (ERA-5) which provides spectral data on a 0.5-degree by 0.5-degree grid around the open boundaries. Sea level data was applied over the nested model domains to allow for the modulation of wave energy over the shallow ebb-tidal delta system. This was sourced from the hydrodynamic model discussed in 3.2. Wind boundary conditions were sourced from NOAA's (National Oceanographic and Atmospheric Administration) global 0.312-degree by 0.312-degree NCEP (National Centre for Environmental Prediction) reanalysis model.

3.4 Model Results

3.4.1 Tidal Currents

A typical spring tidal cycle period was extracted from the 2010 year model run in order to analyse maximum tidal currents and how they would be affected by the construction of a dredge channel (see Figure 3.13 for tidal time-series). Figure 3.14 and Figure 3.15 show that, as per Bell *et al*. (1998), flood tidal velocities in the entrance channel are weaker than ebb tidal currents, which exceeded 2.5 m/s during this spring tide. The strongest differences between Entrance Channel tidal currents in the original and dredged bathymetry were seen during the ebb tide, where for the dredged scenario currents were up to 1.5 m/s greater within the dredge channel and 0.4 m/s lower on the ebb-tidal delta surrounding the channel (frames 10-12 in Figure 3.16). The dredge channel appears to focus the tidal current energy which was previously spread more evenly across the ebb-tidal delta.

Tidal currents at Pukenui were lower than in the Entrance Channel, reaching a maximum of 1.6 m/s on the ebb tide through the Papakura Channel for the original scenario and 1.4 m/s for the dredged scenario (Figure 3.17 and Figure 3.18 respectively). The dredge channel had the opposite effect on tidal currents at Pukenui compared to the ebb-tidal delta, slowing currents by up to 1.8 m/s at the proposed docking area at the end of the dredged channel during both flood and ebb tides (Figure 3.19). This slowing of tidal currents is due to the pre-existing channel being deepened, unlike dredging through the ebb-tidal delta, so the currents that were previously focused through the Papakura Channel now have a greater cross-sectional area to flow through. Results also show localised areas of higher current speeds for the dredged scenario at Pukenui, although these did not exceed 1 m/s.

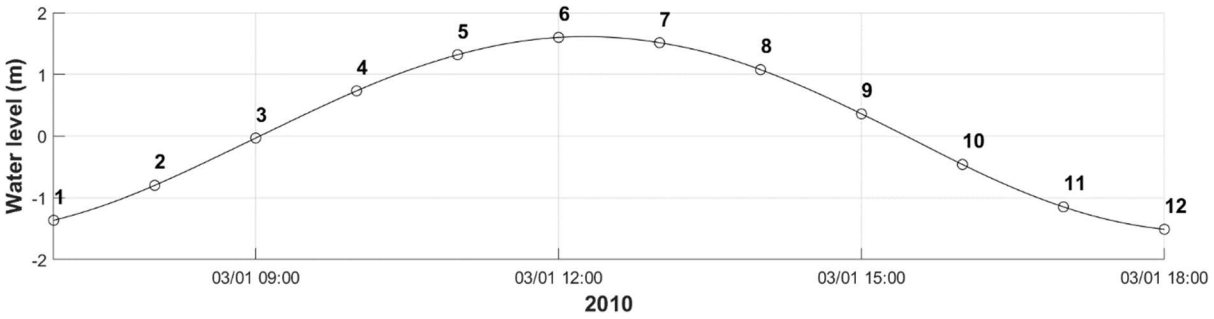

Figure 3.13. Spring-tide time-series extracted from the Manukau Harbour Entrance Channel, numbered every hour on the hour in reference to the frames in the following figures.

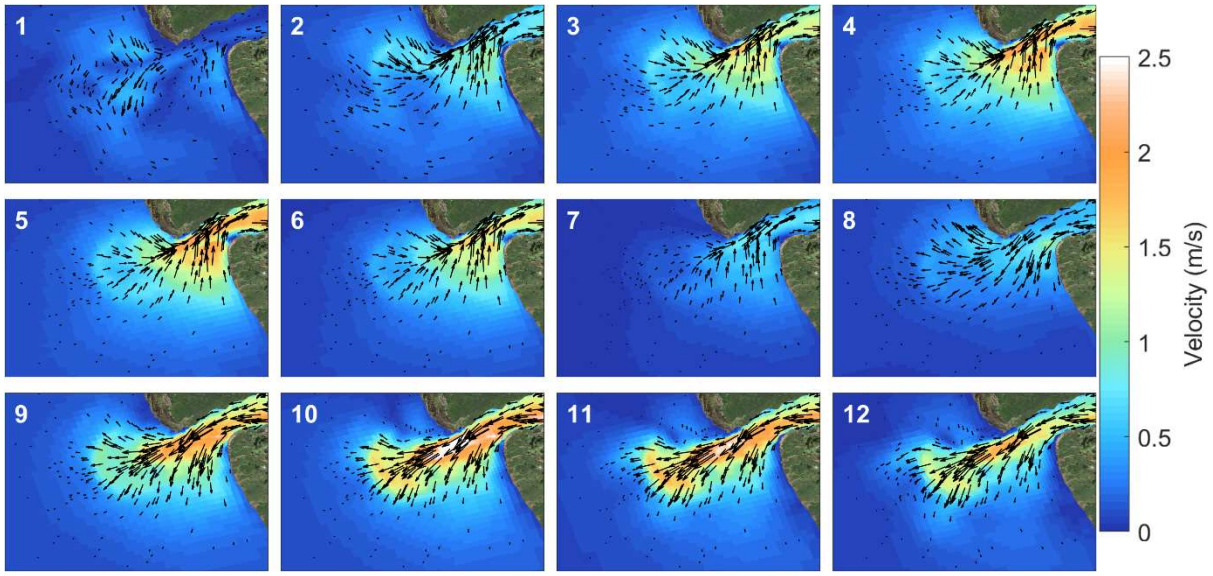

Figure 3.14. Hourly spring-tidal currents at the ebb-tidal delta for the original bathymetry. For time reference see numbers in Figure 3.13.

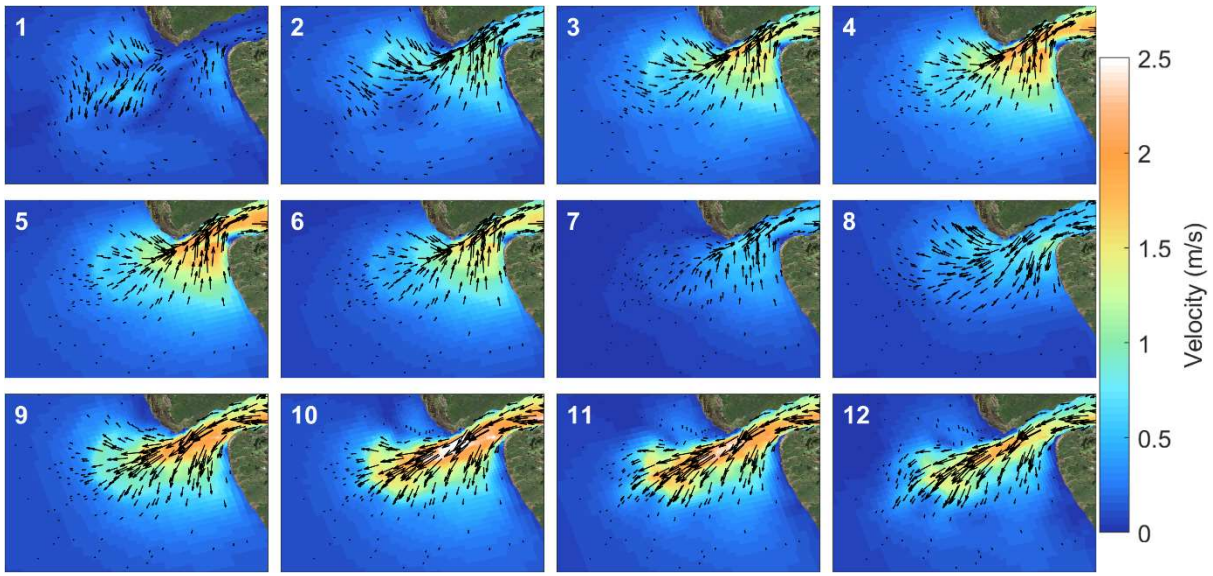

Figure 3.15. Hourly spring-tidal currents at the ebb-tidal delta for the dredged bathymetry. For time reference see numbers in Figure 3.13.

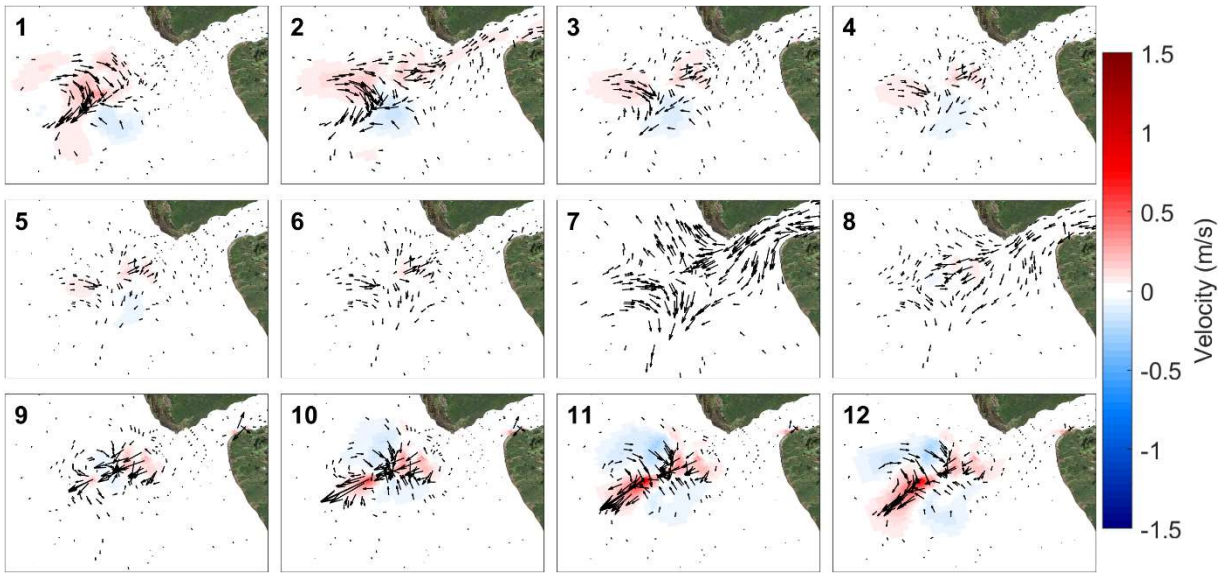

Figure 3.16. Difference between dredged and original bathymetry hourly spring-tidal currents at the ebb-tidal delta. Positive numbers indicate faster currents in the dredged scenario. For time reference see numbers in Figure 3.13.

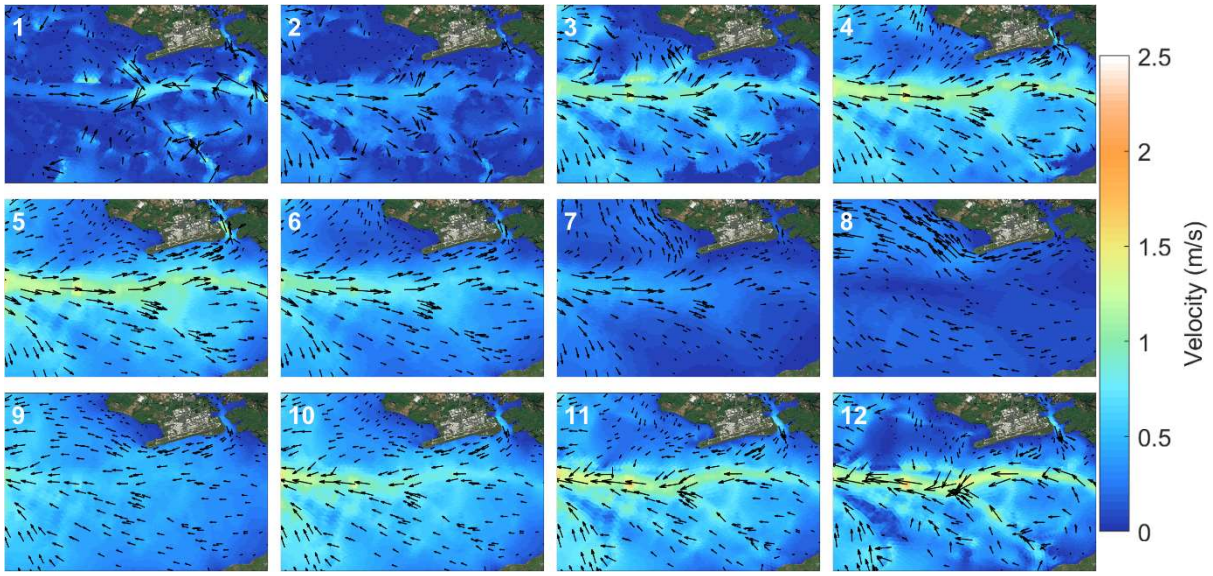

Figure 3.17. Hourly spring-tidal currents at Pukenui for the original bathymetry. For time reference see numbers in Figure 3.13.

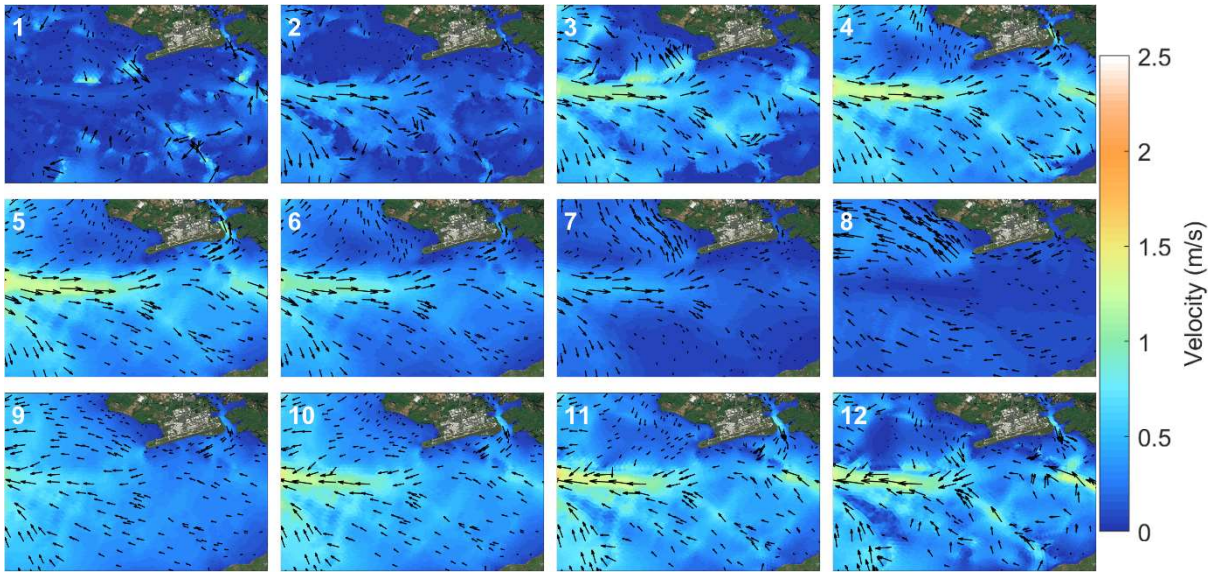

Figure 3.18. Hourly spring-tidal currents at Pukenui for the dredged bathymetry. For time reference see numbers in Figure 3.13.

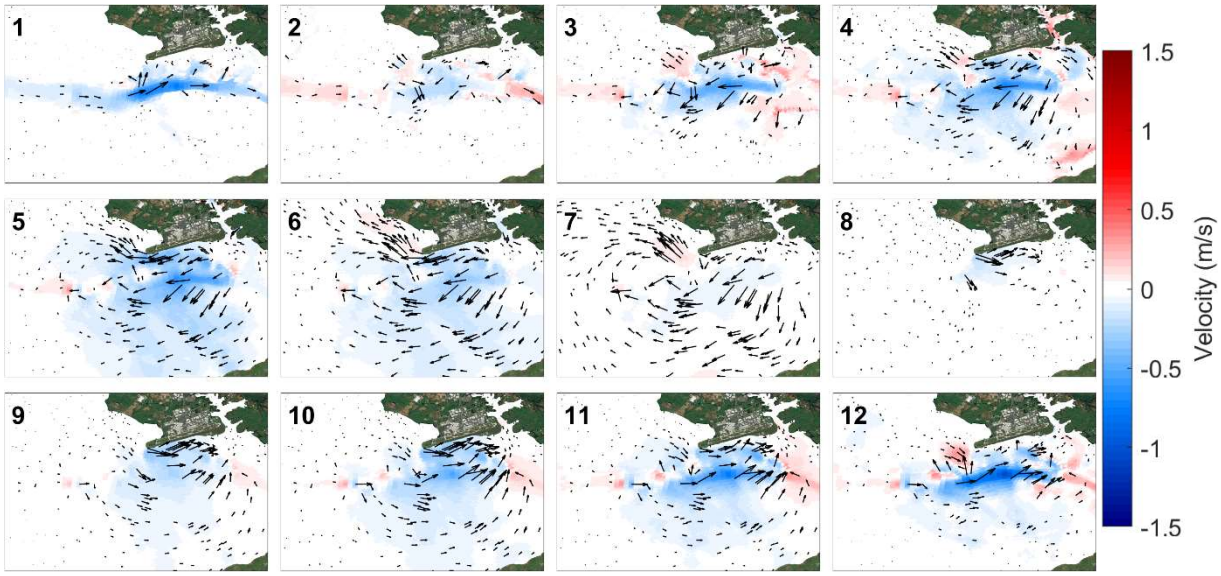

Figure 3.19. Difference between dredged and original bathymetry hourly spring-tidal currents at Pukenui. Positive numbers indicate faster currents in the dredged scenario. For time reference see numbers in Figure 3.13.

3.4.2 Waves

The results of the modelled wave scenarios are illustrated in Figure 3.20 and Figure 3.21 in the form of mean wave height difference plots. These can be interpreted by considering negative values (blue colours) as reduced wave heights post-dredging and positive numbers (red colours) as wave amplification post-dredging.

The year-long model runs (Figure 3.20) which encompass a high energy year (1991), low energy year (2017) and an average year (2010) all show a dampening of waves in the dredge

channel by about 0.8 m on average, which is intuitive since the sea bed has been deepened and therefore wave-shoaling no longer occurs during all but the most extreme wave events. Following dredging, wave amplification can be observed either side of the dredge channel at its seaward end for all modelled years as these locations now focus wave energy which would have previously been spread along the terminal lobe of the ebb tidal delta. There is also a larger region directly to the north of the dredge channel where waves are amplified following dredging in all years modelled. The deepening of the ebb tidal channel alters long wave refraction and the current dredge design appears to create a region of focussed wave energy in this northern portion of the bar.

Interestingly, there is no appreciable difference between the modelled years in terms of the wave damping/amplification patterns, which indicates that the average annual response of the ebb tidal delta to dredging may be similar year to year.

For the extreme events (Figure 3.21), month-long simulations were carried out to capture the wave conditions either side of the peak of the event. Like the mean annual difference plots, wave heights are reduced by about 0.8 m in the dredged channel and amplified on the shallow regions adjacent to it, where waves are focussed post-dredging for all three extreme events modelled. The northwest event of July 1986 shows an overall greater magnitude of wave amplification following dredging, particularly on the north side of the bar when compared to the other two extreme events. This is mostly due to the swell direction of this event being from an oblique angle to the alignment of the ebb tidal delta which faces southwest (the prevailing swell direction). The June 1993 and April 1999 events, while bigger, approach the ebb tidal delta ‘front on’ in line with its orientation, and so wave damping/amplification patterns more closely resemble the annual results.

It should be noted that these results are drawn from an uncalibrated wave model and so spatial patterns and mean wave height differences between the non-dredged and dredged bathymetries should be interpreted with caution.

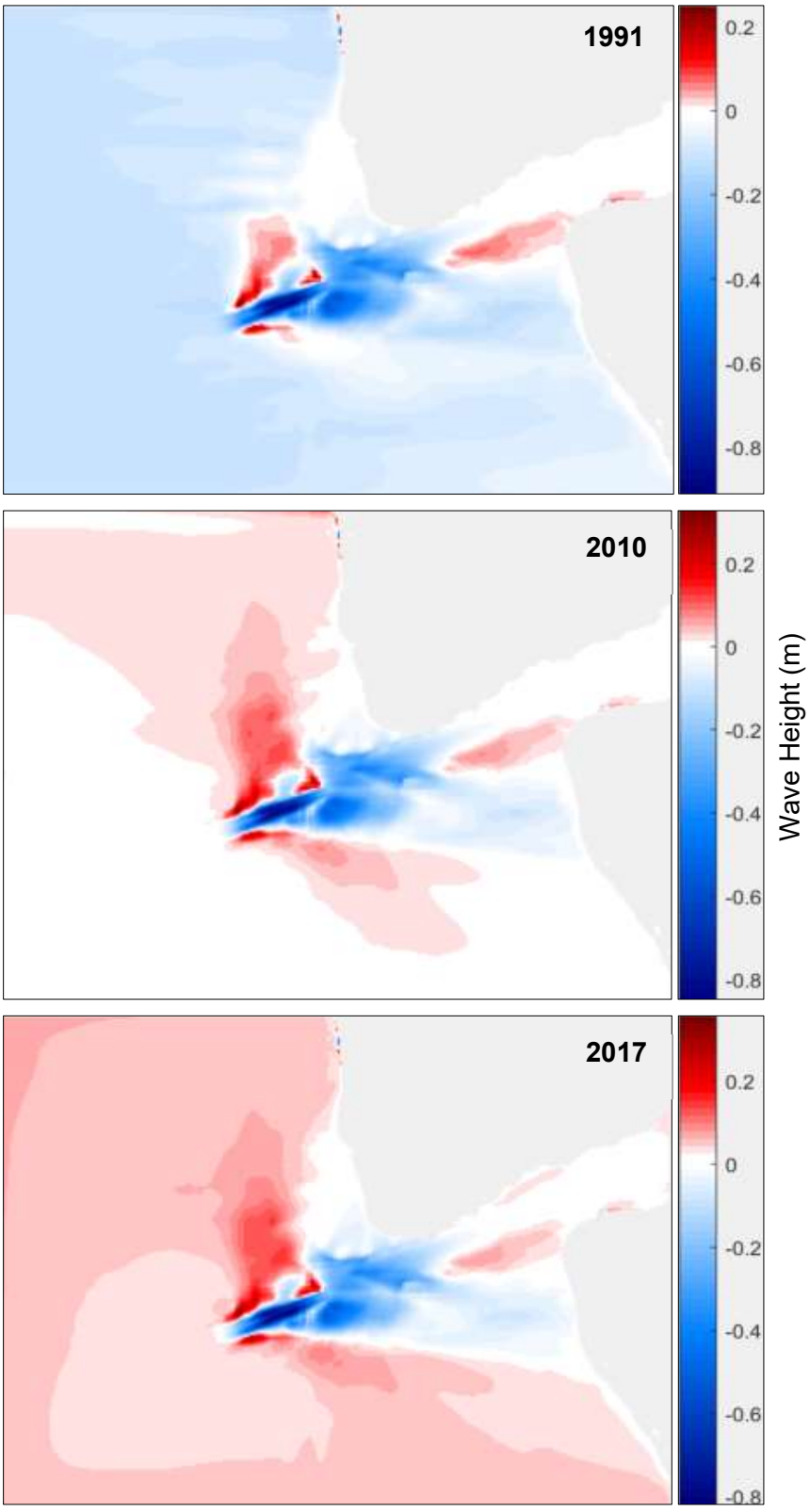

Figure 3.20. Difference between dredged and original bathymetry mean annual wave heights at the ebb-tidal delta. Positive numbers indicate larger wave heights in the dredged scenario.

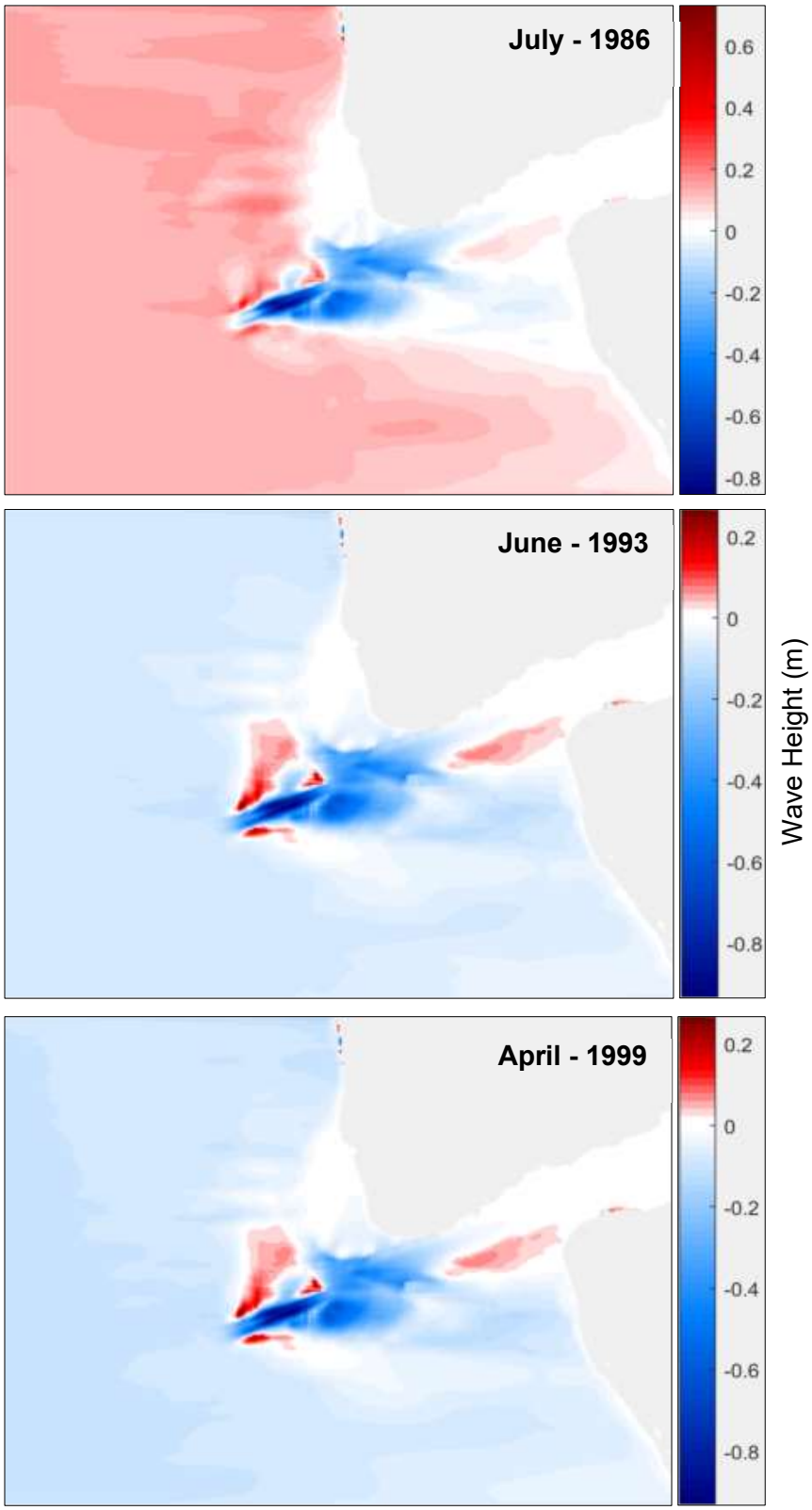

Figure 3.21. Difference between dredged and original bathymetry mean wave heights at the ebb-tidal delta during extreme conditions listed in Table 3.1. Positive numbers indicate larger wave heights in the dredged scenario.

3.5 Annual Dredge Volume Estimations

In order to estimate of the average annual maintenance dredge volumes for the proposed channel, the results from the combined tidal current-wave results from the average year (2010) were converted to sediment transport rate using the methods described in Soulsby (1997). In the absence of a detailed field investigation, several parameters were applied based on previous studies and educated estimates, including d_{50} and d_{90} grain sizes, bed slope β and roughness length z_0. The sediment transport rate was converted to volumes passing through cross-sections on either side of the proposed channel, which were added cumulatively on the condition that the shear stress within the channel was below the critical shear stress for motion at the corresponding time stamp and would therefore be settling on the channel floor.

Sediment grain density was used to define the upper and lower bounds of critical shear stress and therefore volume estimates. Because the actual grain density was unknown, the bounds of 4800 kg/m^{-3} and 5300 kg/m^{-3} were used, which were considered to be a sensible range of grain densities for a typical West Coast titanomagnetite sand. These densities produced critical shear stresses of 0.30 N m^{-2} and 0.33 N m^{-2} respectively, which in turn produced annual maintenance dredge volume estimates of 142,000 m^3 to 214,000 m^2 respectively (Table 3.2). The average annual dredging volume from the 3 years simulated is 178,667 m^3/year.

Table 3.2. Annual maintenance dredge volume estimates for the 3 yearly simulation, and the 3 extreme events. Sediment grain density ρ_s (kg/m^{-3}) of 4,800 and 5,300 for the minimum and maximum, respectively. Critical shear stress for motion τ_{cr} (N m^{-2}) of 0.3 and 0.33 for the minimum and maximum, respectively.

Event	Estimated minimum annual maintenance dredging (m^3)	Estimated maximum annual maintenance dredging (m^3)
2010 (average energy)	150,000	211,000
1991 (high energy)	142,000	199,000
2017 (low energy)	156,000	214,000
July 1986 (northwest)	86,000	125,000
June 1993 (west)	53,000	86,000
April 1999 (southwest)	155,000	208,000

These results indicate that swell direction has a large role in the volumes of channel infilling, since they drive higher rates of alongshore sediment transport, similar to the findings of the literature review (Section 2). For example, even though 1991 was the most energetic year in terms of wave energy in the 40 year dataset, the infilling volumes were estimated to be higher in the lowest energy year due to more wave events from more oblique directions. This is confirmed with the extreme event modelling, where the July 1986 event from the northwest has significantly less energy than the June 1993 event from the west (7.8 m at 13.5 s versus

9.3 m at 14.9 s, respectively), although higher infilling occurred during the northwest event because of the higher incident angle of the waves.

These results also indicate that extreme events likely account for a large proportion of yearly infilling of a channel through the Manukau ebb-tidal delta.

4 Summary and Conclusions

1. This report details uncalibrated numerical modelling that has been undertaken to provide an indication of sedimentation and the impact of extreme storm events on a dredged channel through the Manukau Bar to service a potential Port of Auckland in the Manukau Harbour.
2. In addition, in order to provide further insight into the interpretation of modelling results and likely maintenance requirements, reviews of field investigations and numerical modelling of similar sites (in New Zealand and internationally) were undertaken to provide further information and understanding of the possible dredging regime.
3. All indications are that the ebb tidal delta is in a state of dynamic equilibrium and its shape and the associated orientation of the ebb jet ("Middle Deep") at any given time are in response to longshore sediment supply, incident wave conditions, estuarine sediment supply and tidal forcing.
4. Studies of infilling and maintenance dredging included purely numerical investigations and recorded maintenance dredging. Although there are no sites with close similarity to the Manukau Harbour Entrance, comparison of these studies provides some indication that higher alongshore sediment transport rates result in higher annual dredge volumes, noting this is based on net alongshore sediment transport. It is notable that the Auckland west coast does not have a particular large alongshore sediment rate, even though it is an exposed coast; this is due to the orientation of the coast being almost shore-normal to dominant incident waves from the southwest.
5. Several assumptions have been made for the numerical modelling, some of which may not be valid, although these are unknowns in the absence of site-specific field data. Although no site-specific data were available for model calibration, basic calibration/validation was undertaken using water level data and sensitivity testing was undertaken for horizontal eddy viscosity and uniform bottom friction.
6. Six scenarios were simulated; 3 yearly models representing low, average and high wave energy years, and 3 extreme wave events from 3 different directions (northwest, west and southwest). Models from the Delft3D modelling suites were utilised for the simulations. Wave transformation was undertaken using the wave model SWAN (Simulating WAves Nearshore), and the hydrodynamic (current) modelling utilised D-Flow Flexible Mesh (D-Flow FM). A digitised dredge channel was 15.5 m deep, 250 m wide at the bottom with 1:4 slopes on either side (as considered for the Future Ports Study) and model simulations with and without the dredge channel for the 6 scenarios were undertaken (i.e. 12 model simulations).

7. Model results from D-Flow FM and SWAN were analysed independently and then combined in order to determine their net effect, with model differencing between the existing Manukau Bar and the Manukau Bar with a channel through it applied to sum changes due to the dredging of an entrance channel.
8. In broad terms, the presence of a dredged channel through the Manukau ebb-tidal delta results in increased current velocities through this area of the ebb-tidal delta (by some 1.5 m/s) due to entrainment of the ebb-tidal jet, and reduces currents over the ebb-tidal delta adjacent to the channel. These changes would likely reduce settlement of sediment in the channel and reduce movement of sediment on the ebb-tidal delta (i.e., positive effects for the maintenance of a dredged channel). The opposite occurred for waves, with an average decrease of 0.8 m in the channel (as would be expected with deeper water), and increased wave heights at the inshore end on the sides of the channel due to wave focussing along each side of the channel.
9. Annual dredge volume estimations were calculated using and upper and lower bounds of critical shear stress and therefore infilling volume estimates. Annual maintenance dredge volume estimates of 142,000 m^3 to 214,000 m^3 were determined from the 3 individual year-long simulations, with an overall average of 178,667 m^3/year. Extreme events were estimated to infill the entrance channel from 53,000 m^3 to 208,000 m^3.
10. These results indicate that swell direction has a large role in the volumes of channel infilling, since they drive higher rates of alongshore sediment transport, similar to the findings of the literature review.
11. The average estimated annual infilling/maintenance volume was incorporated into the graph of net alongshore sediment transport rates versus annual dredge volumes from the literature review (Figure 4.1). As can be seen in Figure 4.1, the estimated annual dredge volume for the potential Manukau Harbour entrance channel fits relatively well with the main cluster of data points. Although it is acknowledged that this modelling is a high-level, uncalibrated, estimate of potential channel infilling rates, and that there are a number of limitations and assumptions that may not be valid, this result provides some confidence with respect to the validity of the estimates that have been found.

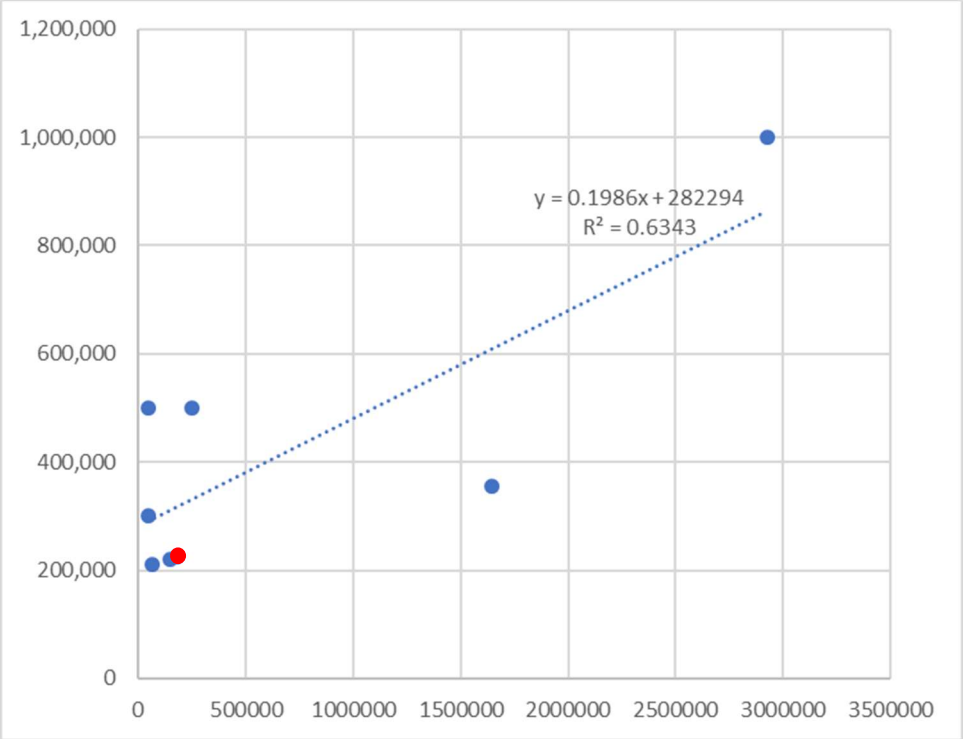

Figure 4.1. Net alongshore sediment transport rates versus annual dredge volumes from Table 2.1, including the average estimated Manukau Heads volume shown in red.

References

Bell, R. G., Sergei V. Dumnov, Bryan L. Williams & Malcolm J. N. Greig (1998). Hydrodynamics of Manukau Harbour, New Zealand, New Zealand Journal of Marine and Freshwater Research, 32:1, 81-100, DOI: 10.1080/00288330.1998.9516807.

Cahill, B. & Lewis, T., (2014). Wave period ratios and the calculation of wave power. In Proceedings of the 2nd Marine Energy Technology Symposium-METS2014, Seattle, WA, USA, 15–17 April 2014.

Castelle, B., Bourget, J., Molnar, N., Strauss, D., Deschamps, S., & Tomlinson, R. (2007). Dynamics of a wave-dominated tidal inlet and influence on adjacent beaches, Currumbin Creek, Gold Coast, Australia. Coastal Engineering, 54(1), 77–90. doi:10.1016/j.coastaleng.2006.08.007.

Chow, V.T., (1959). Open-channel hydraulics. McGraw-Hill Book Co., New York.

Deltares, (2019). D-Flow FM User Manual. version: 1.5.0, July 2019 Published and printed by: Deltares, 402 p. available online: http://oss.deltares.nl/web/delft3d/manuals.

Ernst and Young, 2016. Ports Future Study. Reports prepared for the Port of Auckland Reference Group.

Egbert, G.D., and S.Y. Erofeeva, (2002), Efficient inverse modelling of barotropic ocean tides, J. Atmos. Oceanic Technol., 19(2), 183-204.

Fairburn, T. (1987). The Orpheus Disaster. W.J. Deed Printing Ltd, Waiuku, N.Z. 243p.

Fernández-Fernández, S., Ferreira, C. C., Silva, P. A., Baptista, P., Romão, S., Fontán-Bouzas, Á., Bertin, X. (2019). Assessment of Dredging Scenarios for a Tidal Inlet in a High-Energy Coast. Journal of Marine Science and Engineering, 7(11), 395. doi:10.3390/jmse7110395.

Heath, R. A., Greig, M. J. N., & Shakespeare, B. S. (1977). Circulation and hydrology of Manukau Harbour. New Zealand Journal of Marine and Freshwater Research, 11(3), 589–607. doi:10.1080/00288330.1977.9515697.

Hicks, D.M. and Hume, T.M., 1991. Sand storage at New Zealand tidal inlets. Proceedings, 10th Australasian Conference on Coastal and Ocean Engineering, Auckland, 2-6 December 1991, pp. 213-219.

Hicks, D.M. and Hume, T.M., 1996. Morphology and size of ebb tidal deltas at natural inlets on open-sea and pocket-bay coasts, North Island, New Zealand. Journal of Coastal Research, 12(1), 47-63. Fort Lauderdale (Florida), ISSN 0749-0208.

Holthuijsen, L. H., Booij, N., Ris, R. C., Haagsma, I. J. G., Kieftenburg, A. T. M. M., Kriezi, E. E. & Van der Westhuysen, A. J. (2004). SWAN Cycle III version 40.11 user manual. *Delft University of Technology Press, Delft, The Netherlands*.

Hume, T.M., Bell, R.G., De Lange, W. P., Healy, T. R., Hicks, D. M. and Kirk, R. M. (1992). Coastal Oceanography and Sedimentology in New Zealand, 1967-91. New Zealand Journal of Marine and Freshwater Research.

Kalnay, E., M. Kanamitsu, R. Kistler, W. Collins, D. Deaven, L. Gandin, M. Iredell, S. Saha, G. White, J. Woollen, Y. Zhu, A. Leetmaa, R. Reynolds, M. Chelliah, W. Ebisuzaki, W. Higgins, J. Janowiak, K. C. Mo, C. Ropelewski, J. Wang, R. Jenne, D. Joseph, (1996), The NCEP/NCAR 40-year reanalysis project, Bull. Amer. Meteor. Soc., 77, 437-470.

Kelly, S. (2008). Environmental condition and values of Manukau Harbour. Prepared by Coast and Catchment Ltd. for Auckland Regional Council. Auckland Regional Council Technical Report 2009/112.

McComb, P.J. (2001). Coastal and sediment dynamics in a high-energy, rocky environment. PhD Thesis, University of Waikato, New Zealand. 286 p (plus appendices).

Mccomb, P. J., & Black, K. P. (2000). Port Taranaki maintenance dredging consent renewal studies. Report 1: Field measurements. Volume 1 - Text. Prepared for Westgate Ltd, Port Taranaki, August 2000.

Mead, S. T., 2006. Raglan Extreme Events. Prepared for Waikato District Council, May 2006.

Mead, S. T. and K. P. Black, 1999. A Multi-Purpose, Artificial Reef at Mount Maunganui Beach, New Zealand. Coastal Management Journal 27(4).

Murray-North Ltd (1988). Manukau Harbour Action Plan: Assessment of the recent sedimentation history of the Manukau Harbour. Client report for Auckland Regional Water Board, Murray-North Ltd, Auckland.

NIWA. (2016). New Zealand 250 m gridded bathymetry dataset (https://niwa.co.nz/our-science/oceans/bathymetry).

Pion, L.M., Bernardino, J.C.M. (2018). Dredging Volumes Prediction for the Access Channel of Santos Port Considering Different Design Depths. TransNav, the International Journal on Marine Navigation and Safety of Sea Transportation, Vol. 12, No. 3, doi:10.12716/1001.12.03.09, pp. 505-514.

Pritchard M., Gorman R., Lewis M. (2008). SE Manukau Harbour and Pahurehure Inlet contaminant study: Hydrodynamic, wave and sediment transport fieldwork. NIWA Client Report HAM2008-133, NIWA, Hamilton.

Ramli, A. Y., de Lange, W. P., Bryan, K. R., & Mullarney, J. C. (2015). Coupled flow-wave numerical model in assessing the impact of dredging on the morphology of Matakana Banks. In Australasian Coasts & Ports Conference 2015 (pp. 758-763). IPENZ.

Reed J., Swales A., Ovenden R., Buckthought D., Rush N., Wadhwa S., Okey M.J., Harper S. (2007) South east Manukau Harbour contaminant study. Harbour sediments. NIWA Client Report AK2007-071, NIWA, Auckland.

Reyes-Merlo, M. Á., Ortega-Sánchez, M., Díez-Minguito, M., & Losada, M. A. (2017). Efficient dredging strategy in a tidal inlet based on an energetic approach. Ocean & Coastal Management, 146, 157–169. doi:10.1016/j.ocecoaman.2017.07.002.

Rösler, M. (2015). The Smagorinsky turbulence model. Bachelor thesis at the Institute of Mathematics of Freie Universität Berlin, Research Group Numerical Mathematics and Scientific Computing.

Smith M.J., Stevens C.L., Gorman R.M., McGregor J.A., Neilson C.G. (2001). Wind-wave development across a large shallow intertidal estuary: a case study of Manukau Harbour, New Zealand. N Z J Mar Freshwat Res 35:985-1000.

Soulsby, R. (1997) Dynamics of Marine Sands: A Manual for Practical Applications. Thomas Telford, London.

Trombetta, T. B., Marques, W. C., Guimarães, R. C., de Paula Kirinus, E., da Silva, D. V., Oleinik, P. H., & Isoldi, L. A. (2019). Longshore sediment transport on the Brazilian Continental Shelf. *Scientia Plena*, *15*(4).

Vant, W. N.; Williams, B. L. (1992). Residence Times of Manukau Harbour, New Zealand. New Zealand Journal of Marine and Freshwater Research 26: 393-404.